

## CHAPTER 4

### DATA INTERPRETATION AND DISCUSSION

The efficient use of geophysical methods in environmental applications depends on parameters such as the degree of contamination, thickness of overburden, geological characteristic of the site, areal distribution of soil material, and heterogeneity (Kayabali *et al.*, 1998). Generally, the study expects two kinds of information in groundwater contamination interpretation. The first concerns subsurface conditions and the characteristics of materials below ground surface. The second concerns indirect data regarding the existence of movement of contaminants in groundwater.

The geophysical data analysis and interpretation of resistivity survey data include both the qualitative and quantitative methods. The first method concerns interpretation of the VES curve characteristics. The second method uses the results accomplished from the modeling or inversion program to complete the geological cross section through the available integrated data. In very low frequency electromagnetic data interpretation, the filter plot and relative current density pseudosections can successfully detected lateral variations. Both geophysical methods identify the contaminant plume by low resistivity values.

#### 4.1 Resistivity data interpretation

##### 4.1.1 Qualitative interpretation

The resistivity data analyses began with emphasis on the sounding curves presented in Figure 4.1. The sounding curves of each measurement locations were plotted together on the map. These curves constitute two types. Type 1 curves are

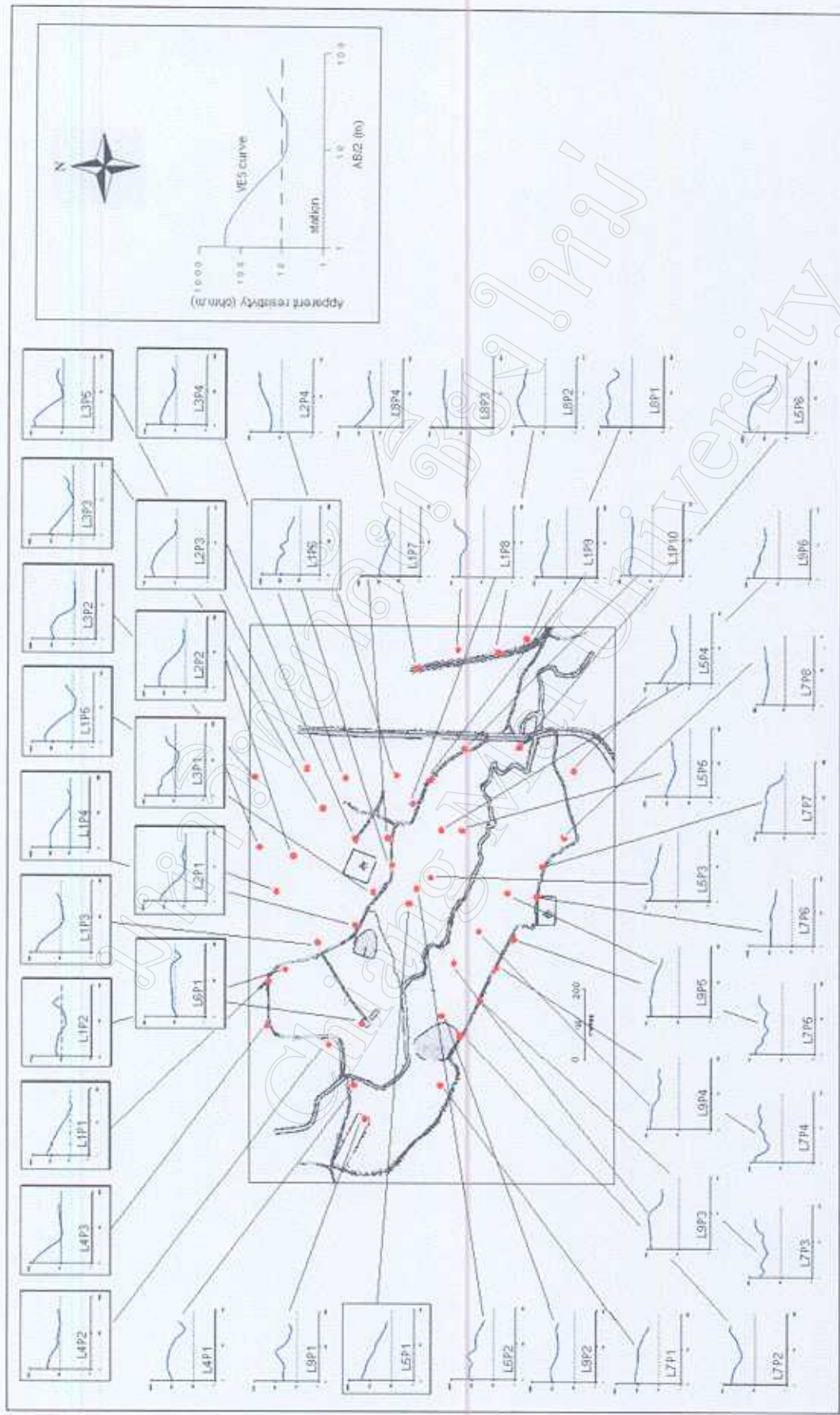


Figure 4.1 Sounding curves of individual resistivity measurement stations.

border curves. The large portions of sounding curves represent the high resistivity layer near the surface. They decrease downward to the intermediate and low resistivity layers. The resistivity then gradually increases with depth. Some curves show that resistivity decrease as the depth increases. The significance character is the minimum resistivity value close to 10 ohm-m reference line. According to data presented in Table 2.1, the resistivity of contaminant plume is 1 to 10 ohm-m. These values are assumed to be the resistivity values of contaminant plume in this qualitative interpretation. Curves of this type occur in the northern part on the study area. Type 2 curves represent the areas that are not contaminated. These curves are characterized by three subtypes. The first subtype has high resistivity near the surface, then decrease downward to the intermediate and low resistivity layers, and finally gradually increase with depth. This subtype curve is the same as type 1 except that the minimum resistivity value is higher than 10 ohm-m. The second subtype shows the resistivity values that decrease with depth and the third subtype shows the resistivity values that increase with depth.

#### 4.1.2 Quantitative interpretation

The quantitative analyses are based on the resistivity model. Four resistivity models are selected to show resistivity variation in different part of the study area. Included are resistivity models at station L6P1, L1P5, L7P2, and L8P2, respectively. All resistivity models are illustrated in Appendix A.

Figure 4.2(a) shows the resistivity model of the station located in the landfill site. All layers have low resistivity values in the range of 2.5 to 16 ohm-m.

Figure 4.2(b) shows the resistivity model of the station located to the east of the landfill. The resistivity of 70.9 ohm-m of the first layer gradually decreases to 34.4 ohm-m in second layer, rapidly drops to 6.5 ohm-m in the third layer, and then gradually increases to 18.4 ohm-m in the fourth layer. The thickness of the low

resistivity layer, 8.8 m, is more than that of the first and second layers, these being 0.9 and 0.7 meters, respectively.

Figure 4.2(c) shows the resistivity model of the station located to the south of the landfill. The high resistivity of 58.8 ohm-m was obtained for the first layer and gradually decreases to 17.4 ohm-m in second layer. The resistivity increases to 97.7 ohm-m and 61.1 ohm-m for the third and fourth layer. The thickness of the third layer is more than that of the first and second layers (0.9 and 0.7 m). Although this model is very similar to that shown in Figure 4.2(b), but the low resistivity value of the low resistivity layer is higher than in Figure 4.2(b).

Figure 4.2(d) shows the resistivity model of the station located to the southeast of the landfill. The resistivity values gradually increase from 31 ohm-m to 38 ohm-m and to 49 ohm-m in the first, second and third layer, respectively, and then drop to 31 ohm-m in the fourth layer. However, in this model the resistivity of individual layer does not change significantly. Each layer can be interpreted to have the same geological characteristics.

Based on resistivity values consideration, the very low resistivity layers displayed in Figure 4.2(a) and Figure 4.2(b) may represent the contaminated zone in the area.

A clearer picture of resistivity modeling of the study area is shown in Figure 4.3. This figure shows the thickness of the earth layers derived from modeling overlain by the resistivity grid color. The first layer has a resistivity greater than 50 ohm-m over nearly all of area and the thickness of 1 to 2 meters. This layer is thinner than the second layer, which is 2 to 10 meters thick, and the third layer, which is 5 to 20 meters thick. The thin layer of the first layer is interpreted to be the overburden and indicated that has no effect of the thickness of overburden in this resistivity survey.

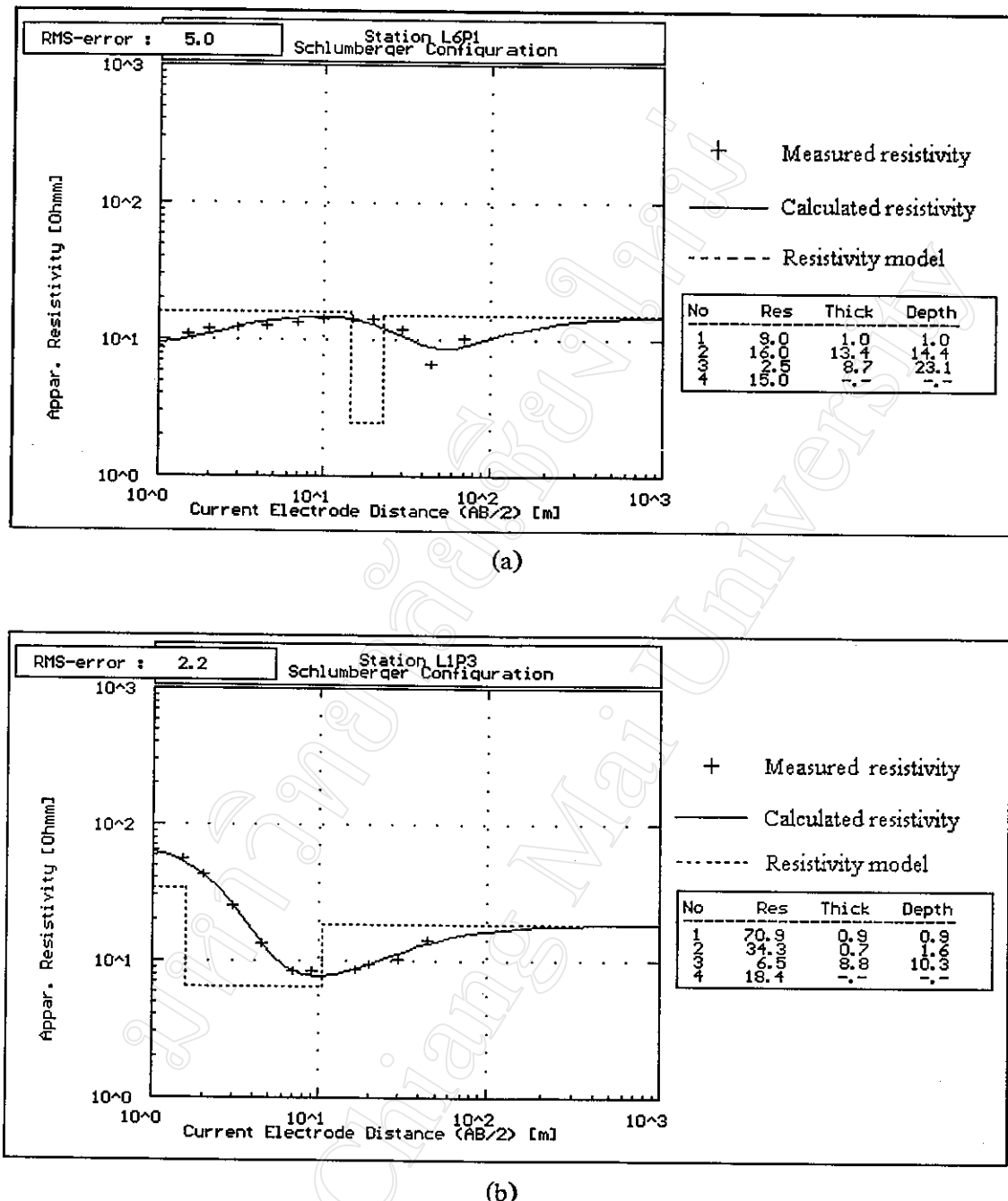
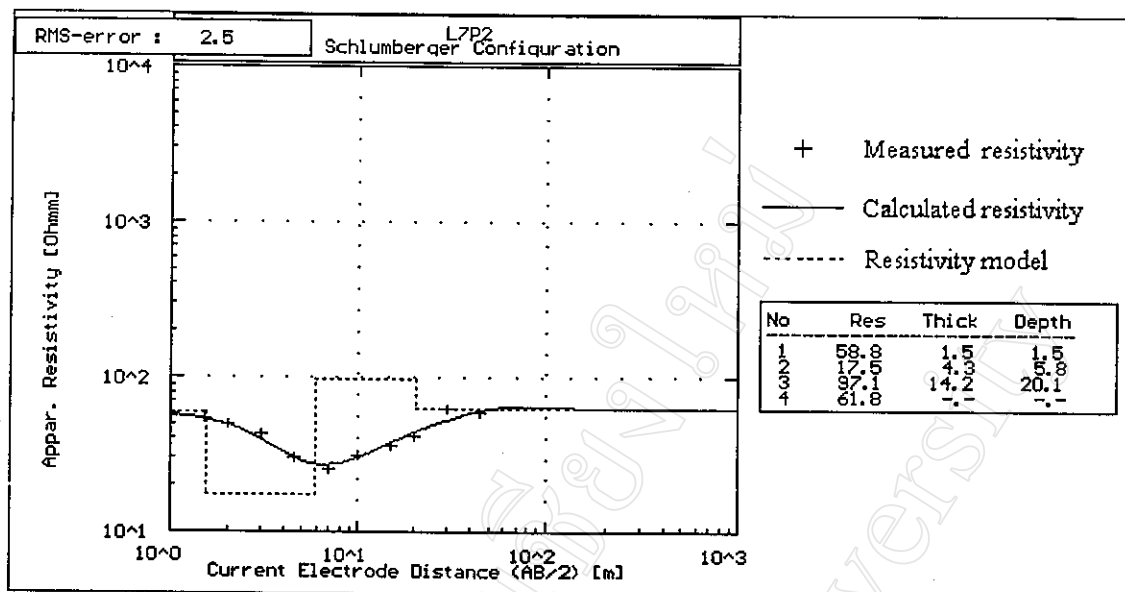
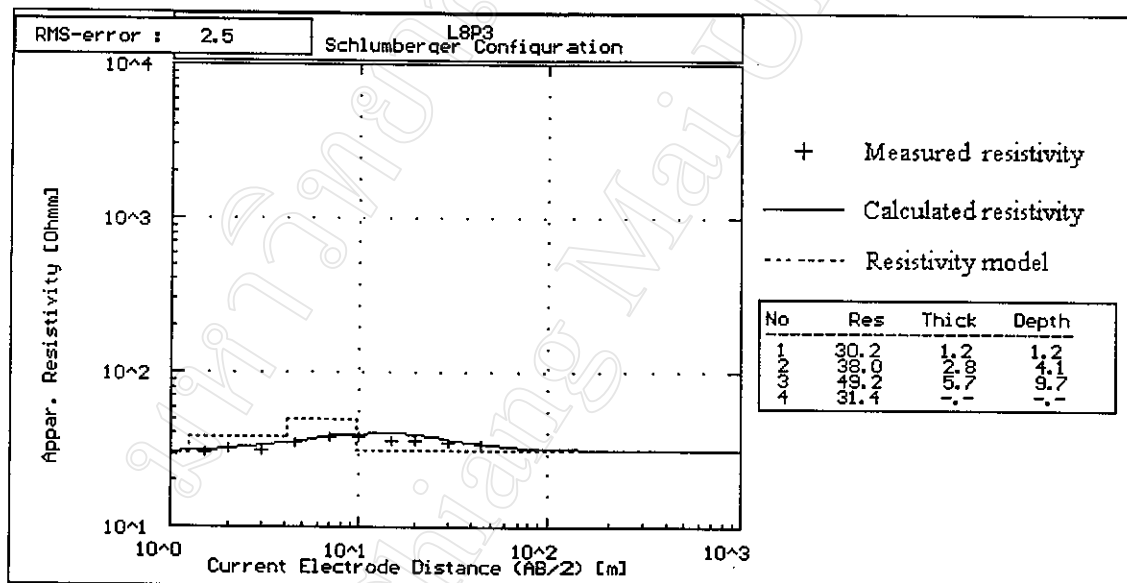


Figure 4.2 Resistivity modeling of station (a) L6P1, (b) L1P3, (c) L7P2, and (d) L8P3.



(c)



(d)

Figure 4.2 (continued).

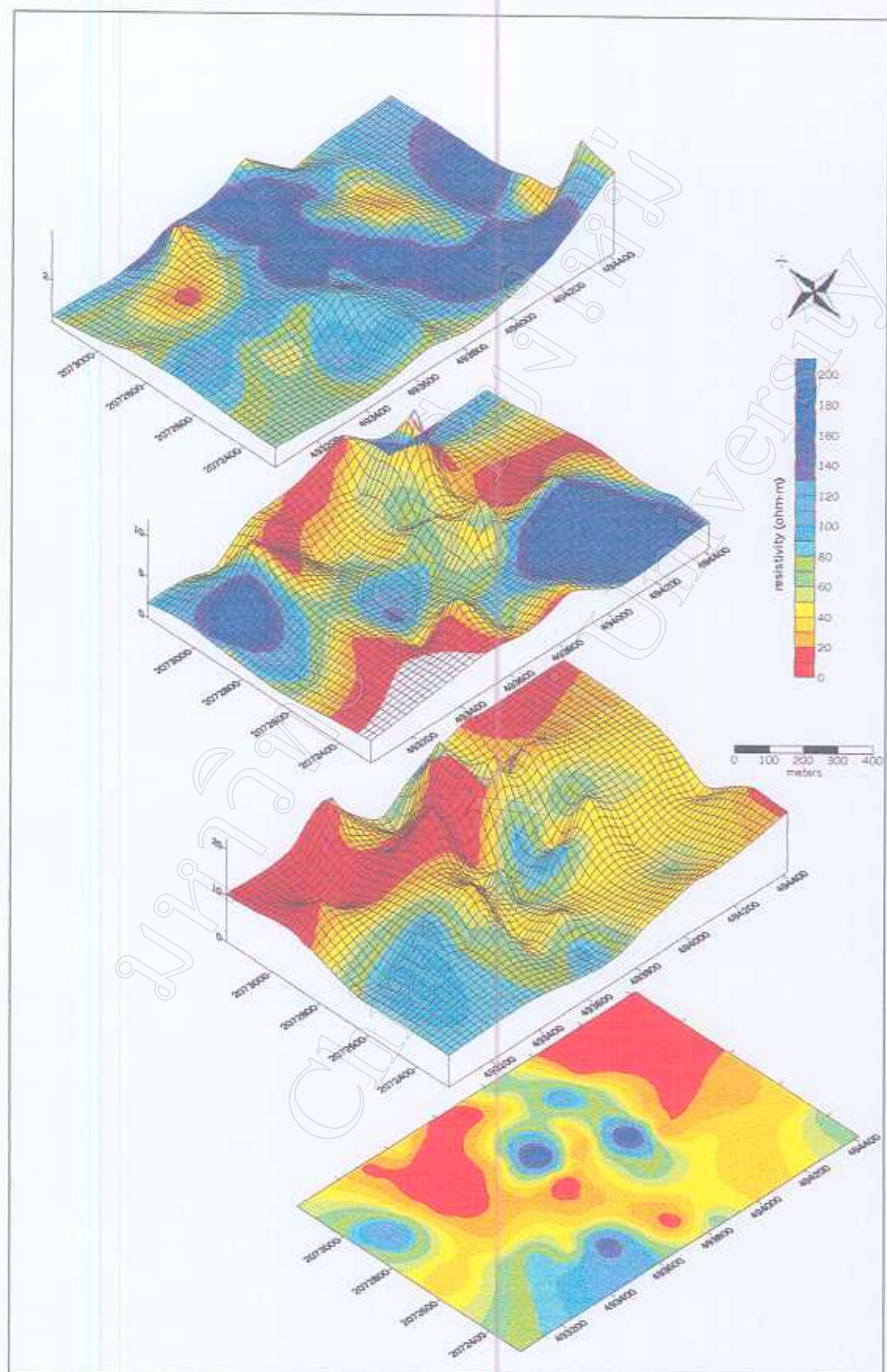


Figure 4.3 The surface plot showing the thickness of layer earth model overlay with resistivity map.

To interpret the resistivity model as a geological model, the relation between resistivity and interpreted geology are illustrated in Table 4.1. Commonly, sand/gravel units display moderate to high resistivity value, whereas fine sediments and waste material show low resistivity value. Resistivities are expected to decrease as water content increase, especially when the sediments have high clay or silt components. Depending on the relative proportion of fluids and/or metallic objects within the landfill, the waste and leachate plume may be locally very conductive. The low resistivity zone of 20 ohm-m was interpreted to be the contaminated area because the existence of low resistivity value (<20 ohm-m) in all layers as shown in Figure 4.2(a). Resistivity modeling of the station located in the landfill suggested that the large portions of subsurface materials are the waste or leachate not fine-grained sediments. The resistivity value of fine-grained materials in Chiang Mai basin obtained from DC resistivity survey and well logging is about 50 ohm-m (Fongsaward S. Singharajwarapan, pers. com., 2001)

Table 4.1 The summary of interpreted geology from geophysical parameters.

Interpreted geology	Resistivity (ohm-m)	Relative current density (%)
Overburden	>20	
Dry sand	>200	Low
Sand and gravel saturated with relatively good quality water	50-200	Intermediate
Fine-grained materials, silts or clays	<50	High
Sand or clay saturated with poor quality (high TDS) water	<20	High

#### 4.1.3 Resistivity maps at selected elevations

Maps of resistivity at a particular elevation are generated by sampling the sounding interpretations at depths determined by a modeling program. The resistivities are sampled at 297, 295, 293, 291, 289, 287, 285, 283, 281, and 279 meters above mean sea level, respectively. The resultant sampled resistivities and the corresponding location values are gridded using an interpolating program to construct the resistivity maps as shown in Figure 4.4(a) to Figure 4.4(j). This presentation form easily determines lateral variation.

Figure 4.4(a), 4.4(b) and 4.4(c) are the resistivity maps at the elevation of 297, 295 and 293 meters above mean sea level, respectively. These elevations correspond to the depth of about 1-10, 1-12 and 1-14 meters below surface, respectively. The western part is deeper than the eastern part of site. These maps show the continuous broad pattern of low resistivity zone (less than 20 ohm-m) that were shaded by red color. The zones extend in west to east. An area of moderate to high resistivity appeared in the southern and western part of the site.

Figure 4.4(d) and 4.4(e) are the maps at the elevation of 291 and 289 meters above mean sea level, respectively. Low resistivity zones are still appeared in these maps but the zones are gradually narrower and separated into 2 parts, one is lied beneath landfill site 1 and the other is lied beneath landfill site 2 with extend from northwest to southeast.

Figure 4.4(f), 4.4(g), 4.4(h), 4.4(i) and 4.4(j) are the resistivity maps of 287, 285, 283, 281 and 279 meters above mean sea level, respectively. These maps show significance change of low resistivity zone pattern, whereas the moderate to high resistivity zones patterns are quite same. Low resistivity zone under landfill site 1 extends in 2 directions, northeastward and southeastward. The distinctive appearance of the trend of low resistivity zone in southeast can be seen at the elevations of 287 to 283 meters and trend of low resistivity zone in northeast can be seen at the elevations

of 285 to 279 meters. The low resistivity zone under landfill site 2 is not presented but the trend of low resistivity zone are displayed in the east of site 2.

The low resistivity anomalies in the northern part of the landfill as shown in Figure 4.4(a), 4.4(b) and 4.4(c) are interesting in that they may have two sources of contamination. The contaminant plume of landfill site 1 migrated eastward and blended with contaminant plume of site 2, and then they migrated together. It is possible that there is a rise in the water table under the landfill and these low resistivity values are water quality related. At the elevations from 291 to 289 meters, the contaminant plume are limited and lied under the landfill sites. At the elevations between 287 and 279 meters, the large portions of contaminant plume caused by landfill site 1 and migrated in northeast and southeast direction. An extension of contaminant plume in southeast may caused by the channel that run through the study area. The middle and southern parts of the site that show moderate to high resistivity values of 30 to 120 ohm-m from coherent zones or trends may be caused by fine grain deposits.

Figure 4.5 is a series of depth slice sections that shows the extent of low resistivity zones that are interpreted as contamination zones. These depth slices clearly present the boundaries of contamination zone by red color shading. They indicate that the continuous contaminant plume may be appeared from elevation of 297 meters to 293 meters (surface to 14 meters depth) and migrate eastward. The contaminant plumes are spilt at the elevation of 291 meters to 289 meters (16 to 18 meters depth), and then the contaminant plume has migrated from landfill site 1 to the northeastern and southeastern parts of the site. The gradual increase in the resistivity values away from the landfill implies that the contaminant plume is either becoming less conductive (i.e. less contaminated) or that it is thinner. The contaminant plume is restricted to the leachate seepage point at the landfill site with limited extension both in vertical and horizontal directions.

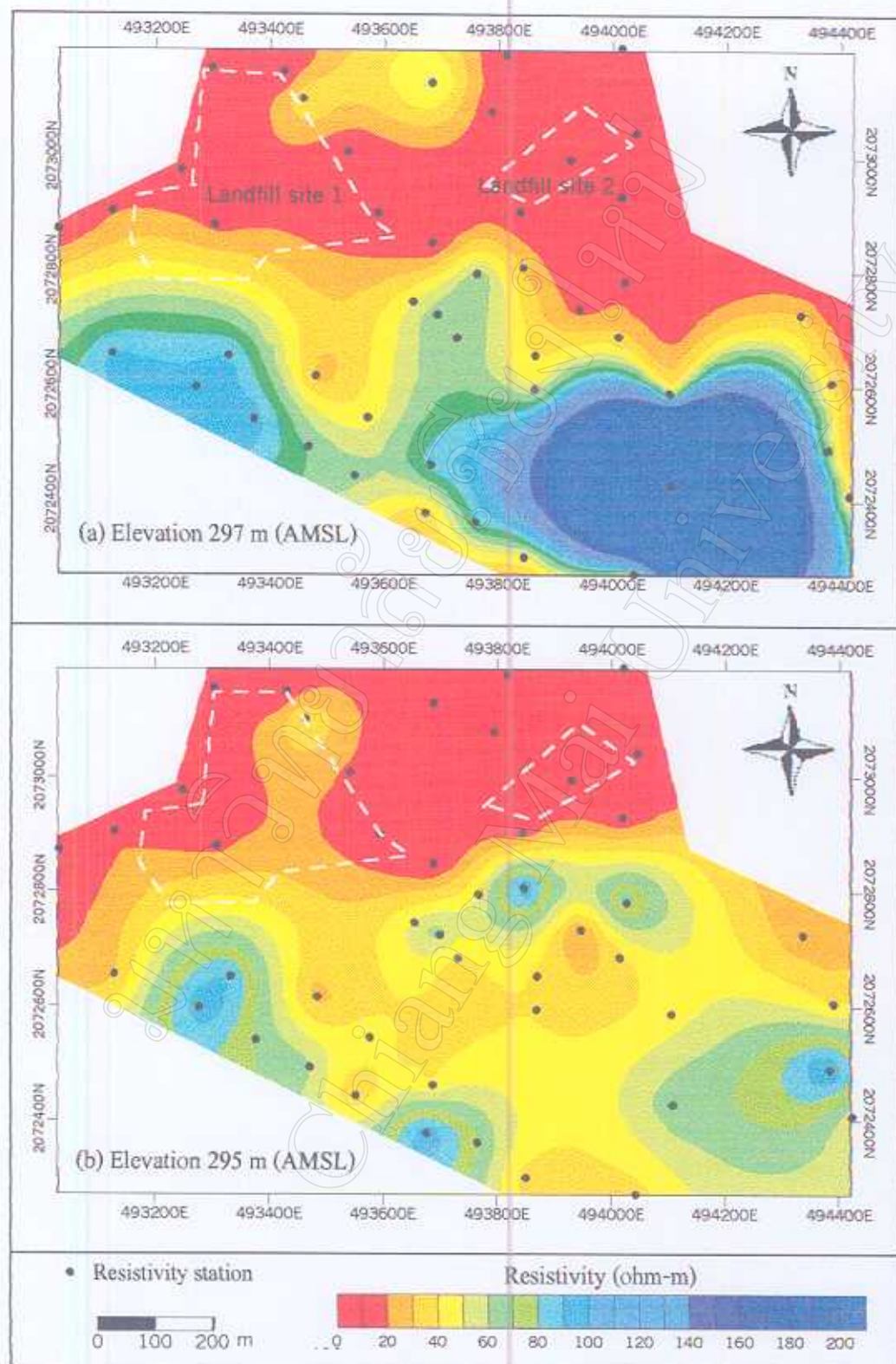


Figure 4.4 Resistivity map at different elevations (a) 297 m, (b) 295 m, (c) 293 m, (d) 291 m, (e) 289 m, (f) 287 m, (g) 285 m, (h) 283 m, (i) 281 m, and (j) 279 m.

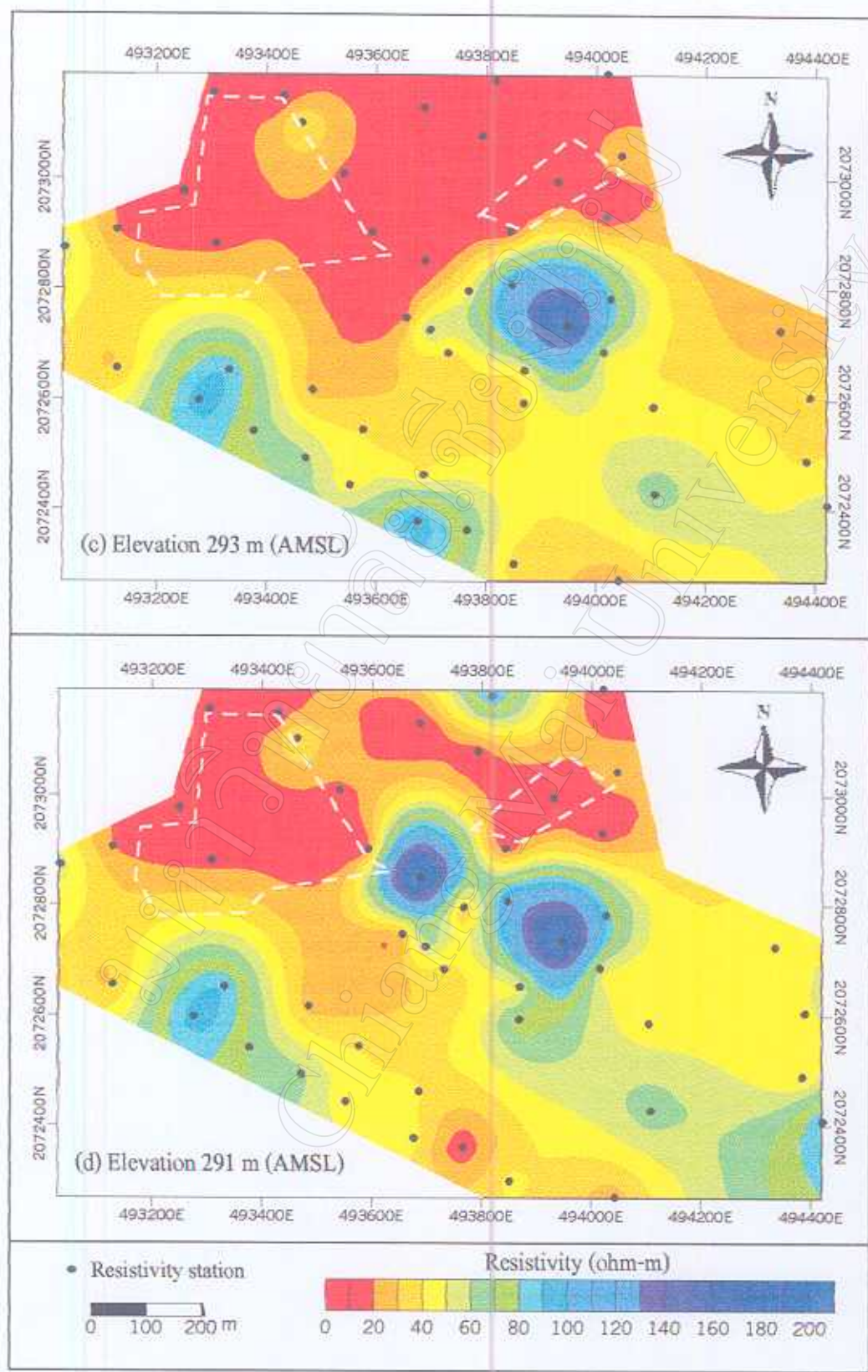


Figure 4.4 (continued).

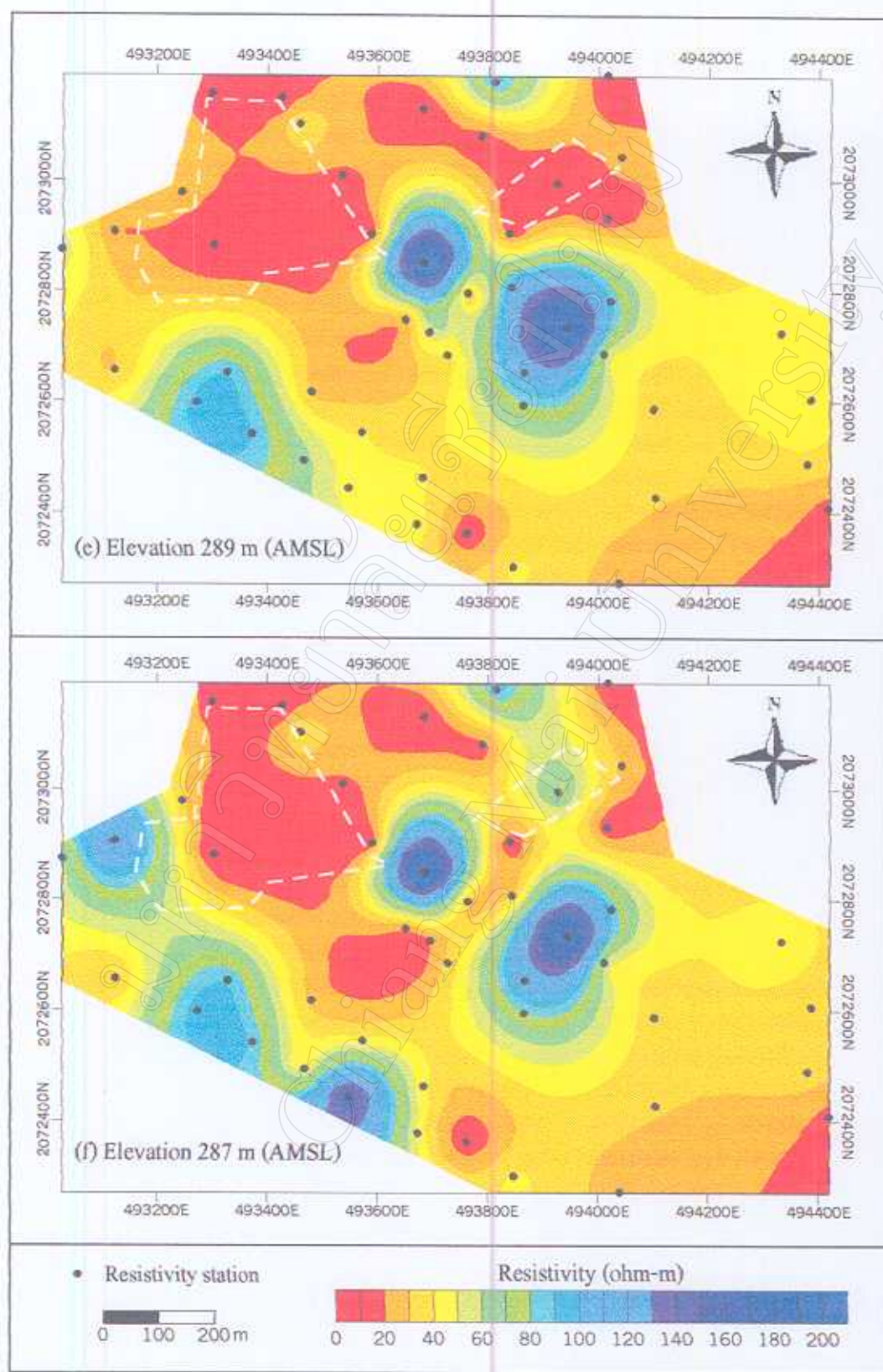


Figure 4.4 (continued).

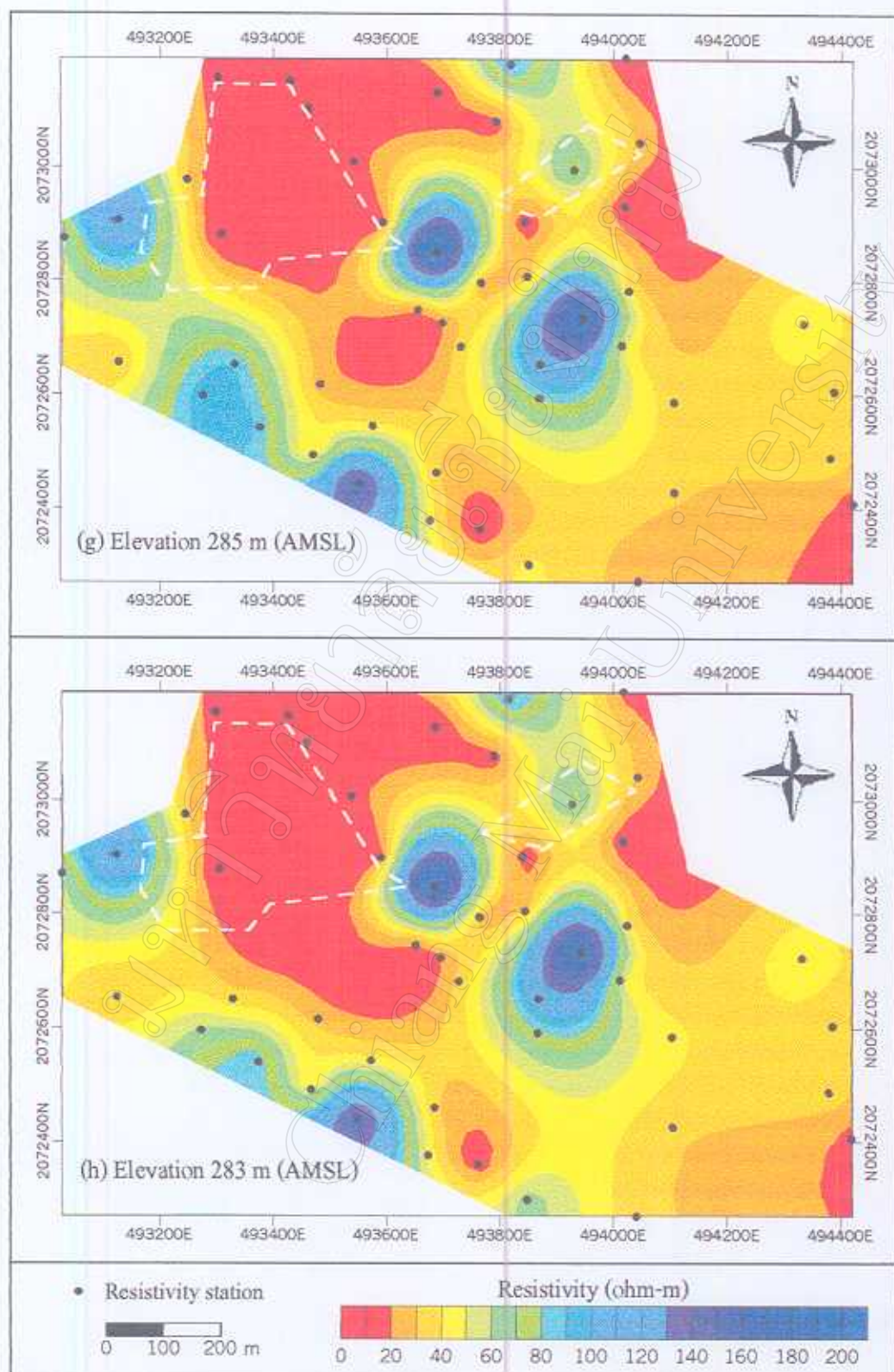


Figure 4.4 (continued).

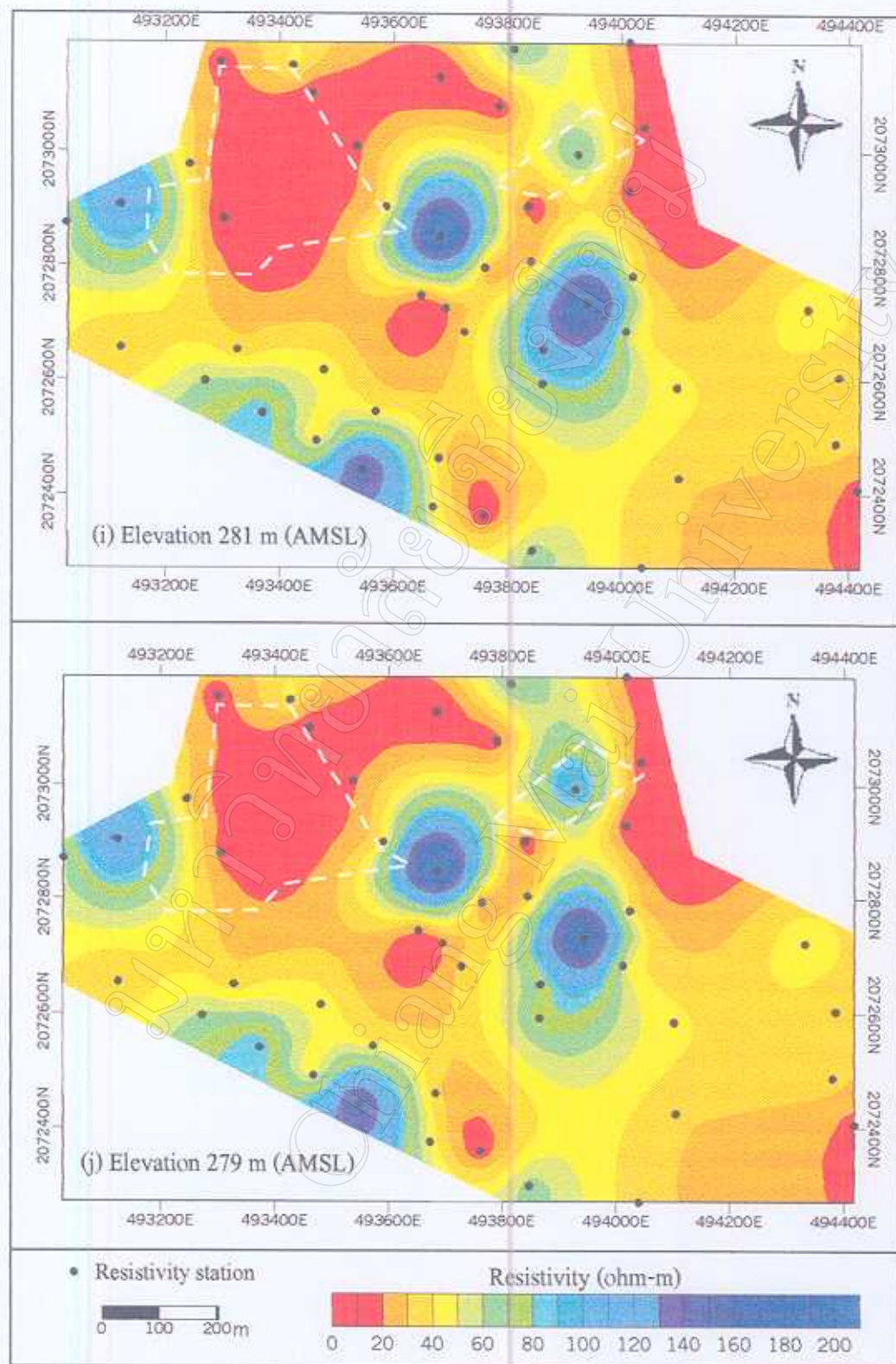
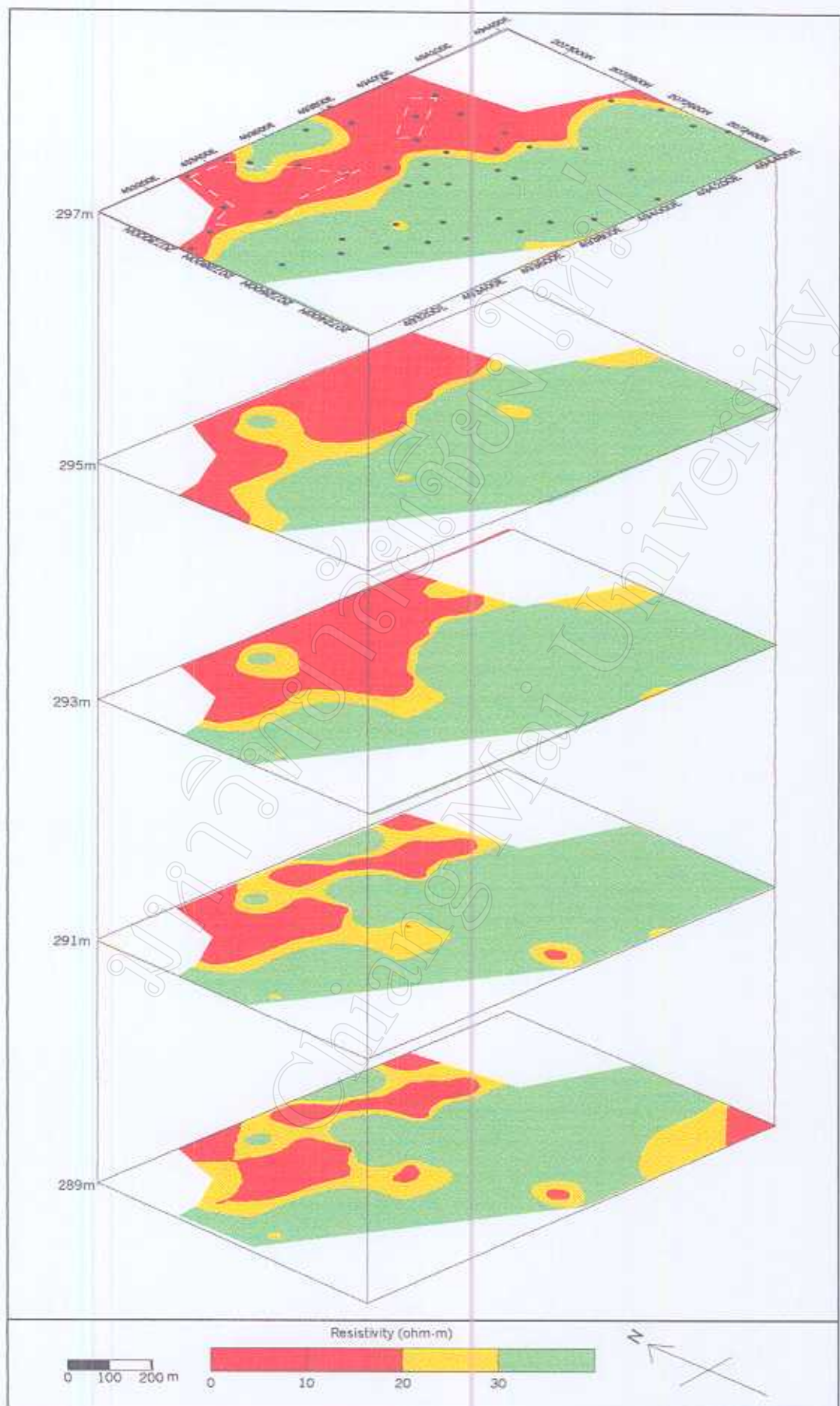


Figure 4.4 (continued).



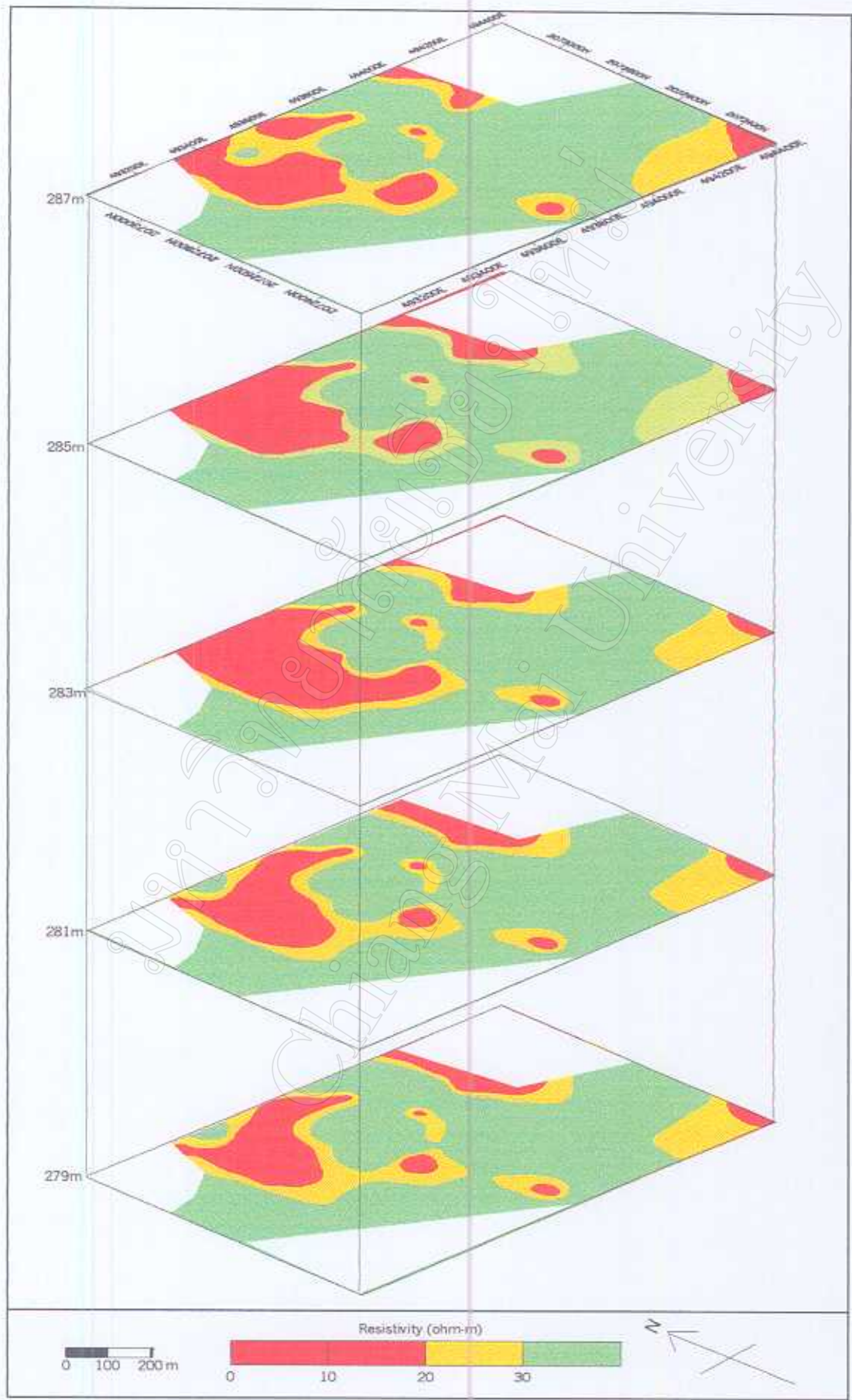


Figure 4.5 (continued).

#### 4.1.4 Electrical resistivity profile

Resistivity profiles oriented east-west and north-south directions were constructed to describe the boundaries of contaminated zone in terms of vertical variation. These profiles are shown in Figure 4.6.

Figure 4.7 shows the resistivity profiles oriented in east-west direction. These profiles are arranged from the northeast to the southwest. Profile AA', BB' and profile CC' show that the low resistivity zone (<20 ohm-m) occurs in the western part of profiles with the thickness of 5-15 meters. The low resistivity zones are existed near the landfill site 1. They can be interpreted that contaminant plume may be migrated from landfill to the east in the groundwater flow direction and possibly downward into a deeper aquifer. The westernmost profile DD', may represents an uncontaminated zone.

Figure 4.8 shows north-south oriented resistivity profiles. Profile EE' through profile KK' are arranged from the northwest to the southeast. Profile EE', FF', GG' and HH' represented contaminated zone in the eastern part of each profile. The uncontaminated area is in the southeast of study area and can be inferred from profile II'.

The geologic cross sections as interpreted from resistivity data are presented in Figure 4.9 and Figure 4.10. There is no borehole data in the study area. The available borehole data of well located nearby the study area is shown in Figure 4.11. It shows that at depth less than 25 meters, thin sand and gravel lens or layers are interbedded with the predominant clayey sediments. Consequently, The interpreted contaminant plume that lied adjacent to the limited area of sand and gravel layer may be the contaminated area in sand and gravel lens.

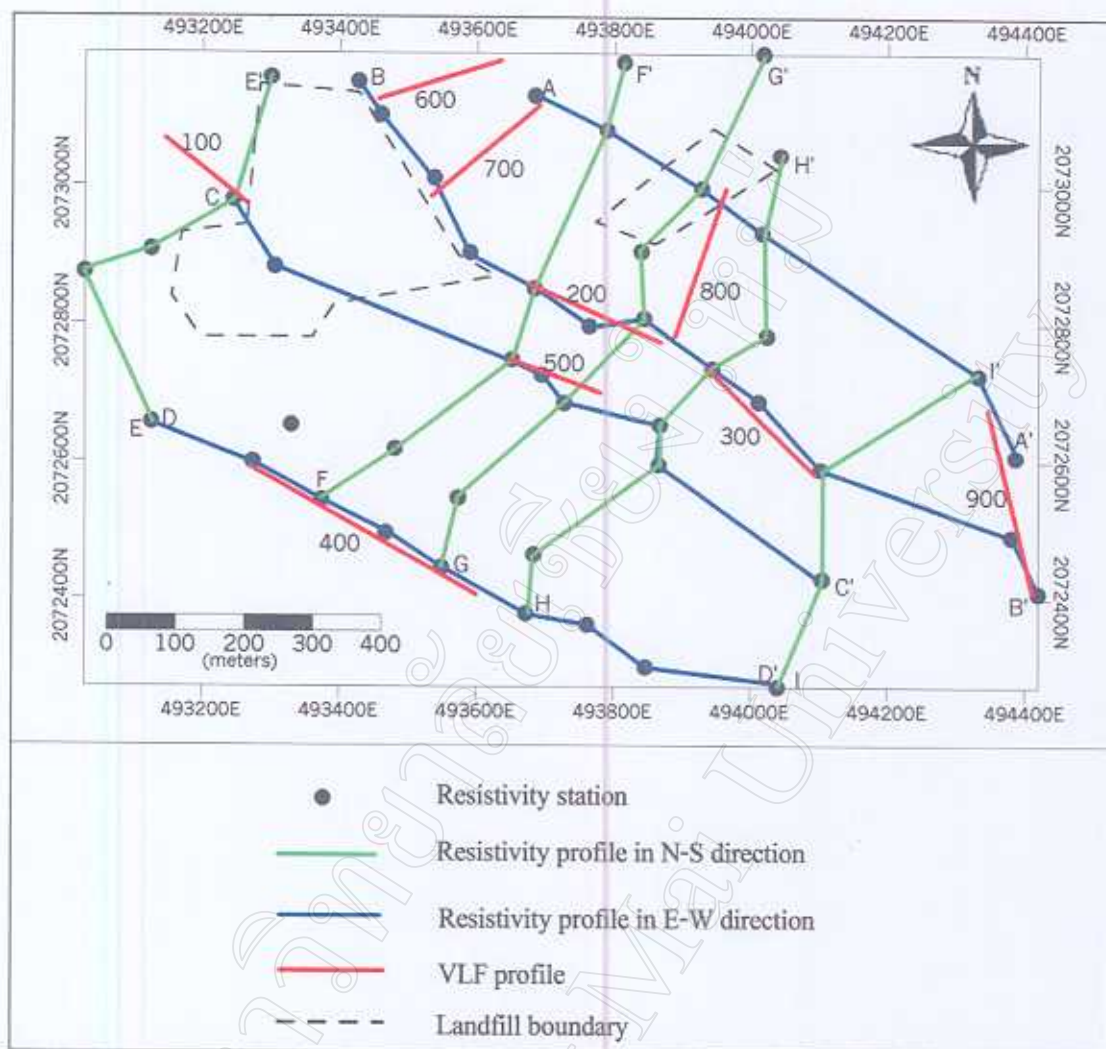


Figure 4.6 Map showing resistivity and VLF profiles.

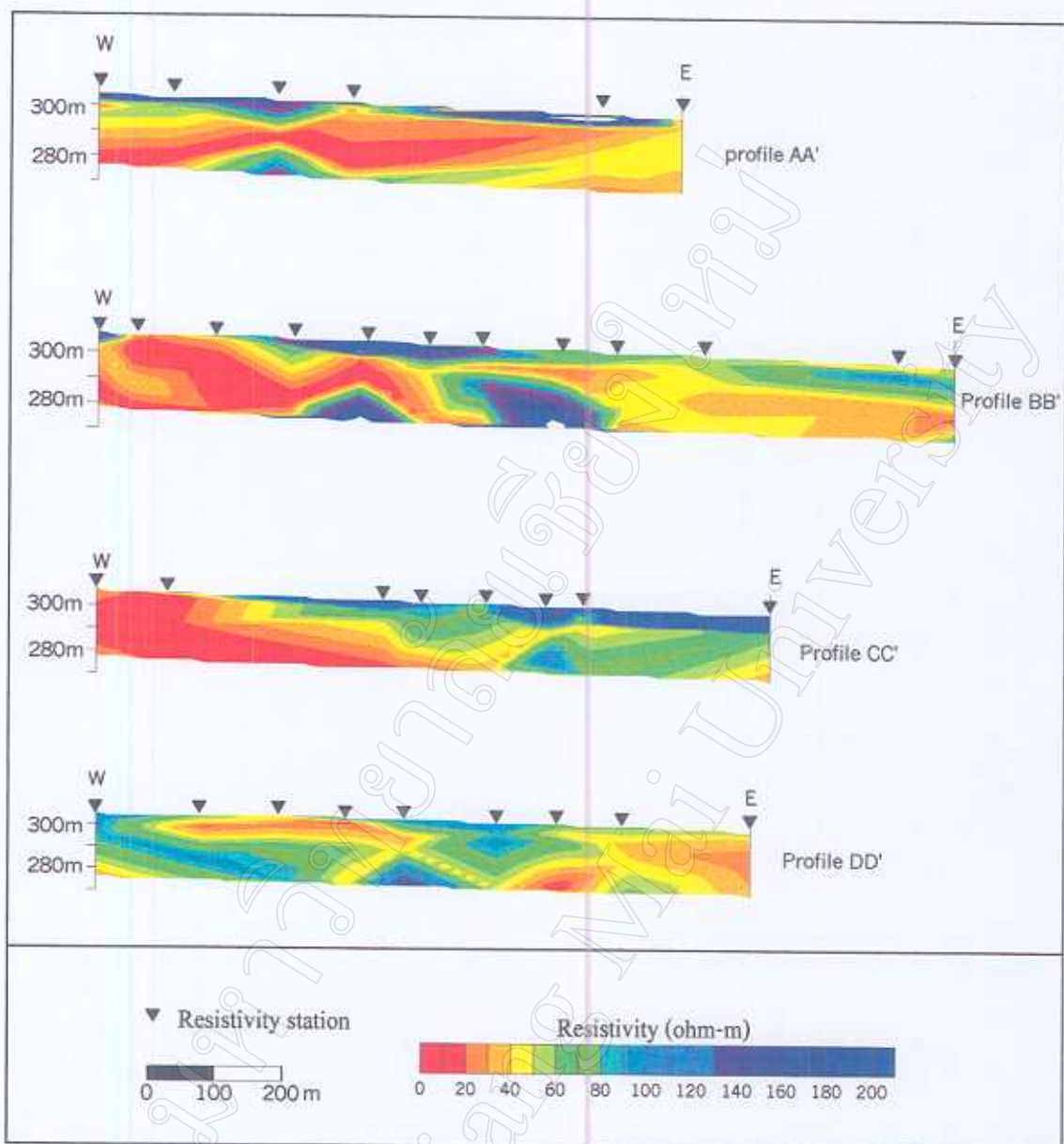


Figure 4.7 Resistivity profiles in east-west direction.

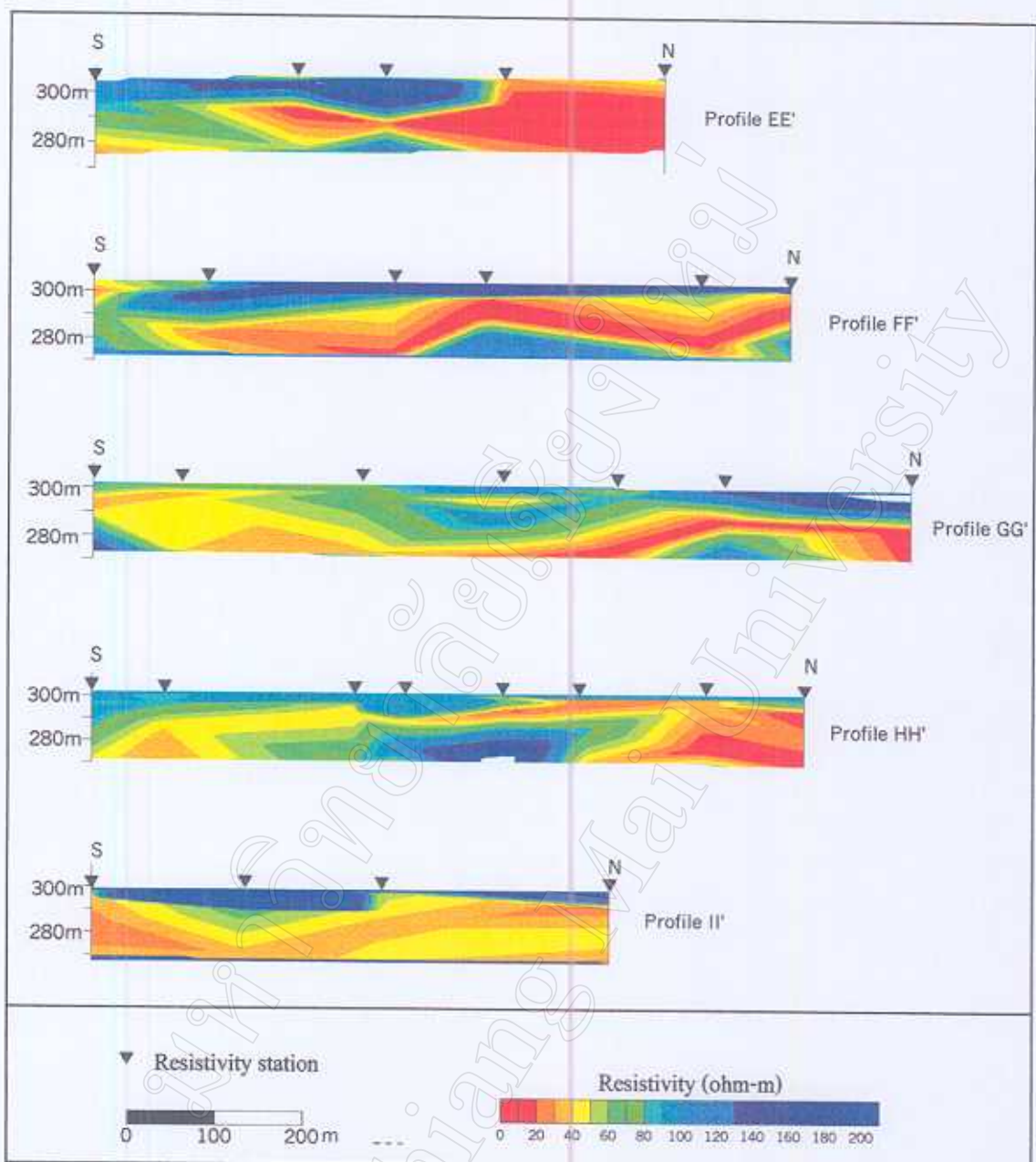


Figure 4.8 Resistivity profiles in north-south direction.

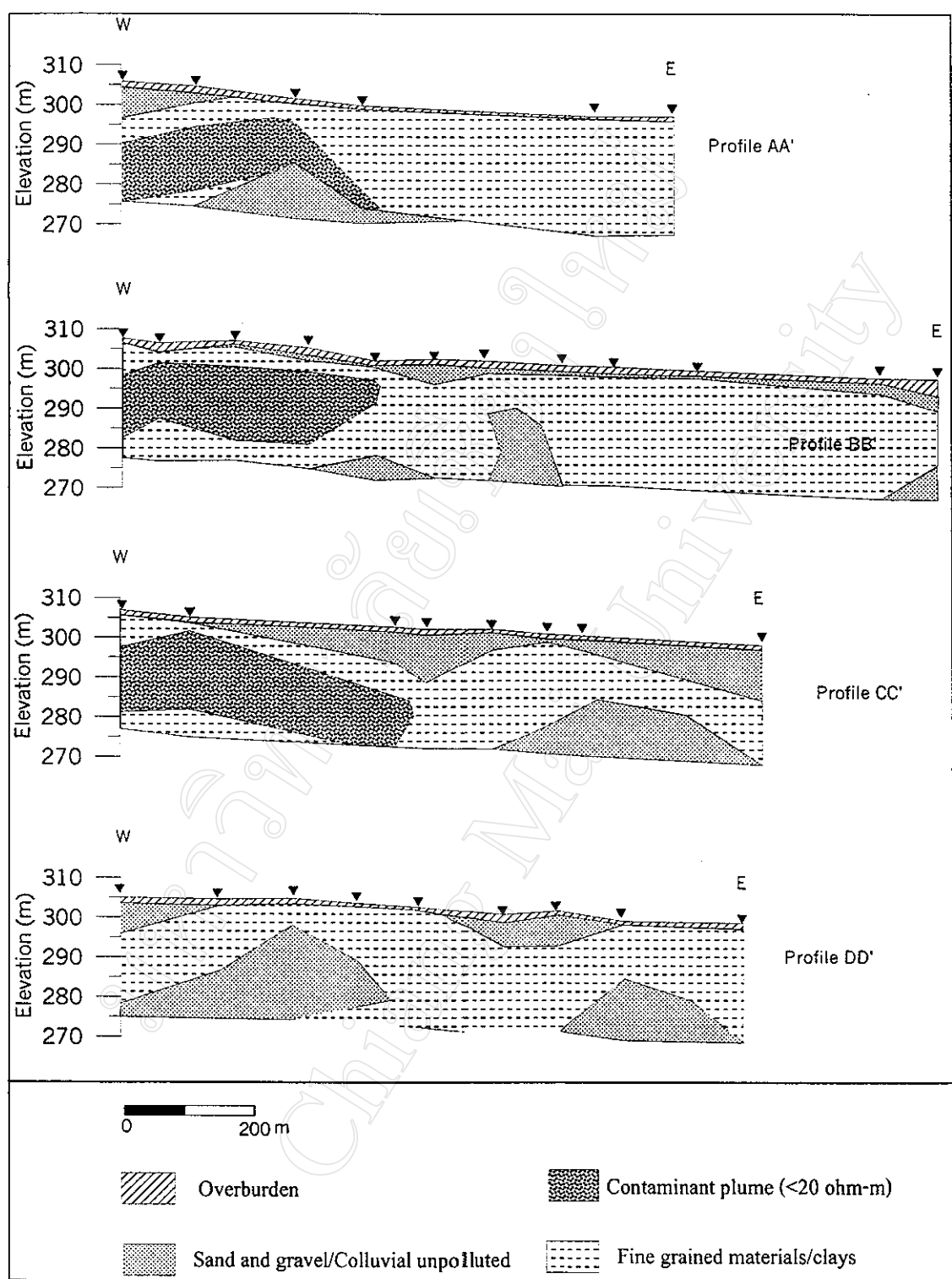


Figure 4.9 Schematic geologic cross section in east-west direction as interpreted using resistivity data.

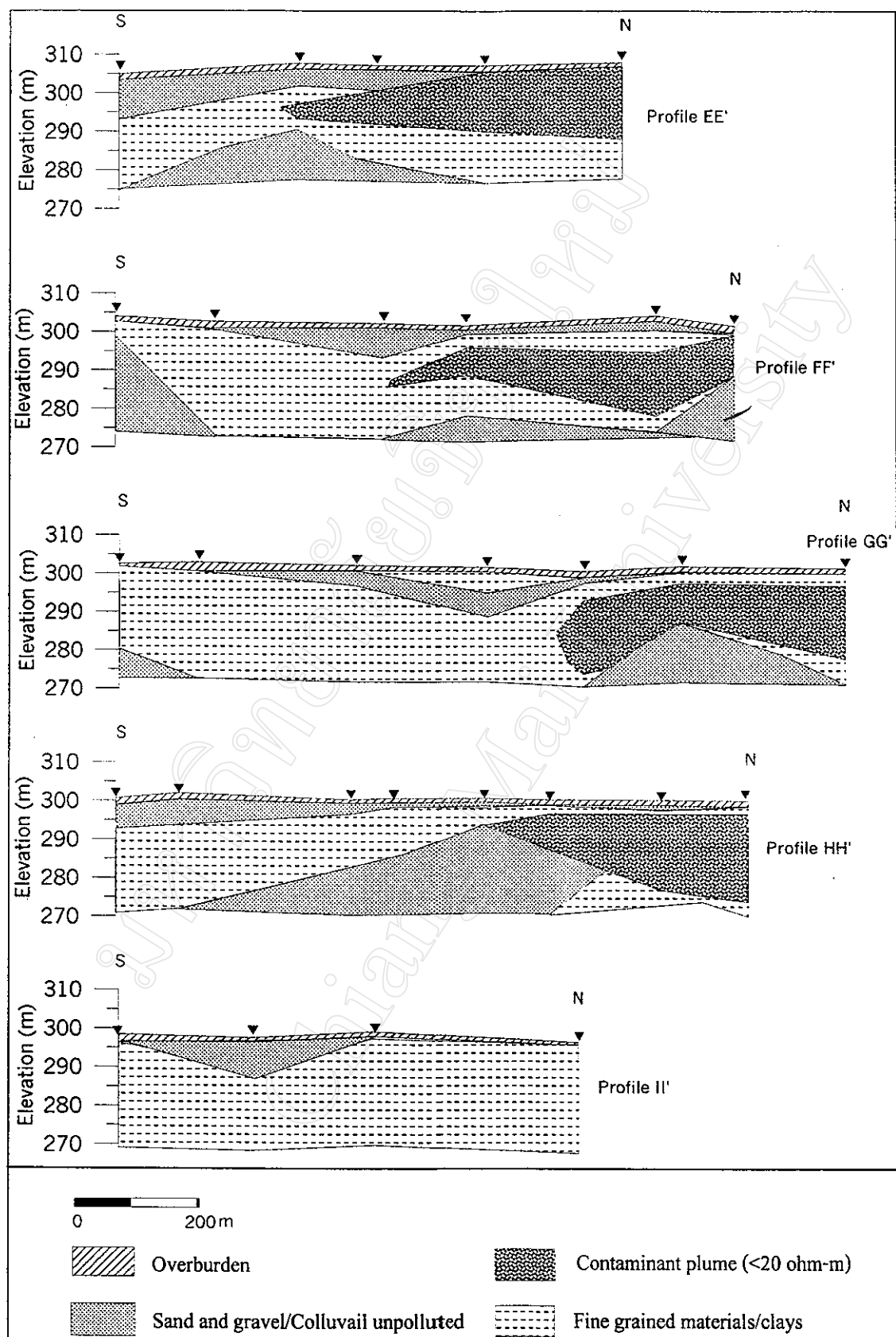


Figure 4.10 Schematic geologic cross section in north-south direction as interpreted using resistivity data.

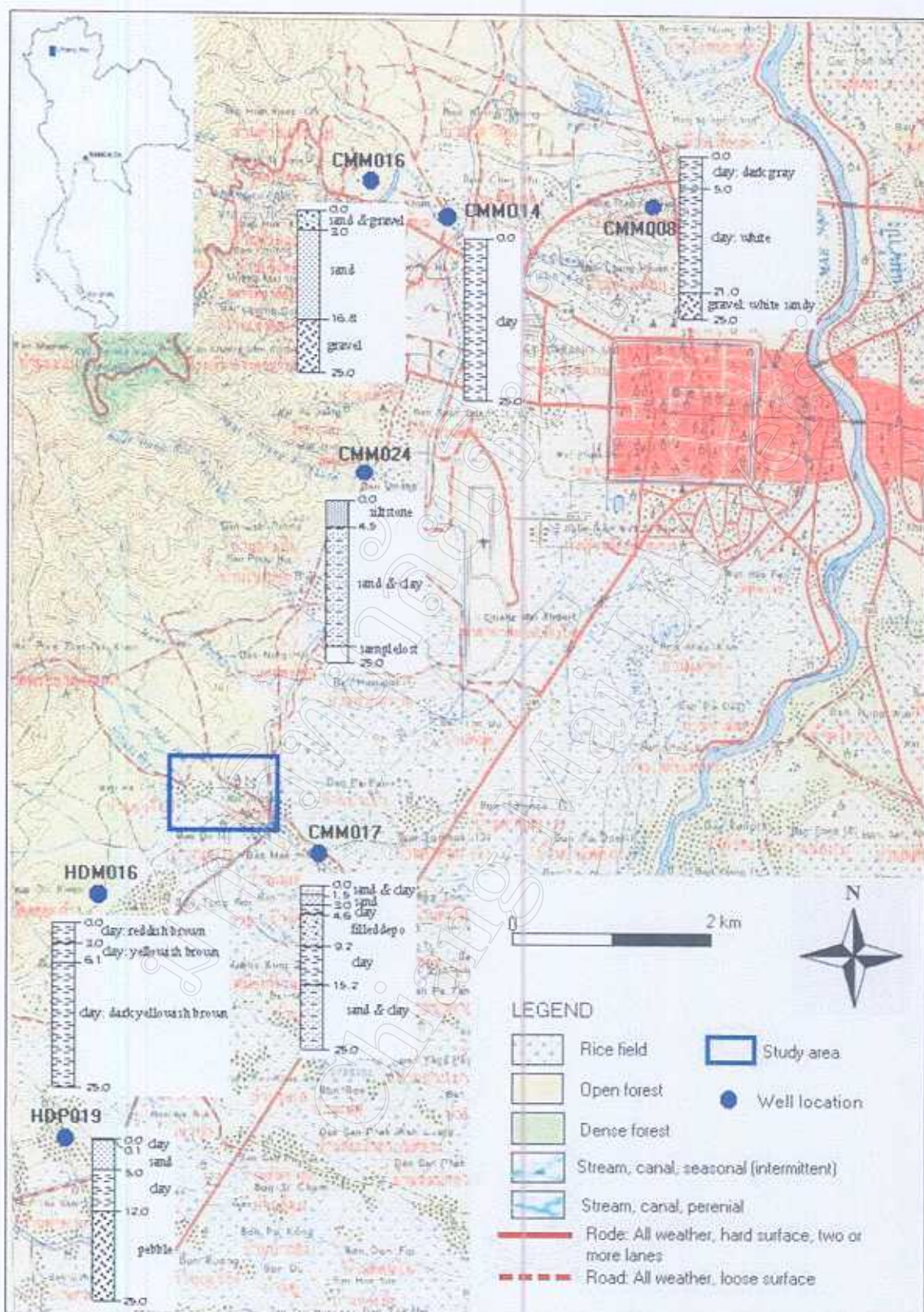


Figure 4.11 Map showing borehole data of wells located near the study area

(data from Tatong *et al.*, 1997a ; 1997b).

## 4.2 Very low frequency electromagnetic data interpretation

Very low frequency electromagnetic data interpretation based on an original data plot, a filtered plot and a relative current density pseudosection of in-phase component. The following hypothetical idea of interpretation is the resistivity contrast between contamination saturated zone and uncontamination zone may give rise to the change on very low frequency electromagnetic signal. Some original plots, filtered plots and current density pseudosections of lines, which were not run along resistivity profiles, are shown in this part and the others will be shown in the next part for comparison with resistivity profiles.

Figure 4.12(a) through Figure 4.12(e) show data plots of very low frequency profiles 100, 600, 700, 800 and 900, respectively. These profiles are difficult to interpret because the original data plots have negative peaks. The low quality of data may be caused by sources of noise, such as power lines and/or clay layer that is conductive zone near the surface.

## 4.3 Integrated data interpretation

Some very low frequency electromagnetic survey lines are located along selected resistivity profile. These current density pseudosections were plotted with resistivity profiles for comparison, as shown in Figure 4.13, 4.14, and 4.15.

Figure 4.13 shows the comparison of resistivity profile BB' and current density pseudosection of profile 200 and 300. The distinct correlation of profile 200 can be seen in the right end of profile. The low current density zone occurs at the same area as the high resistivity zone in the resistivity profile. In addition, the distinct correlation of profile 300 can be seen in the left end of profile.

Figure 4.14 and Figure 4.15 show the comparison of resistivity profile CC' and current density pseudosection of profile 400 and the comparison of resistivity profile

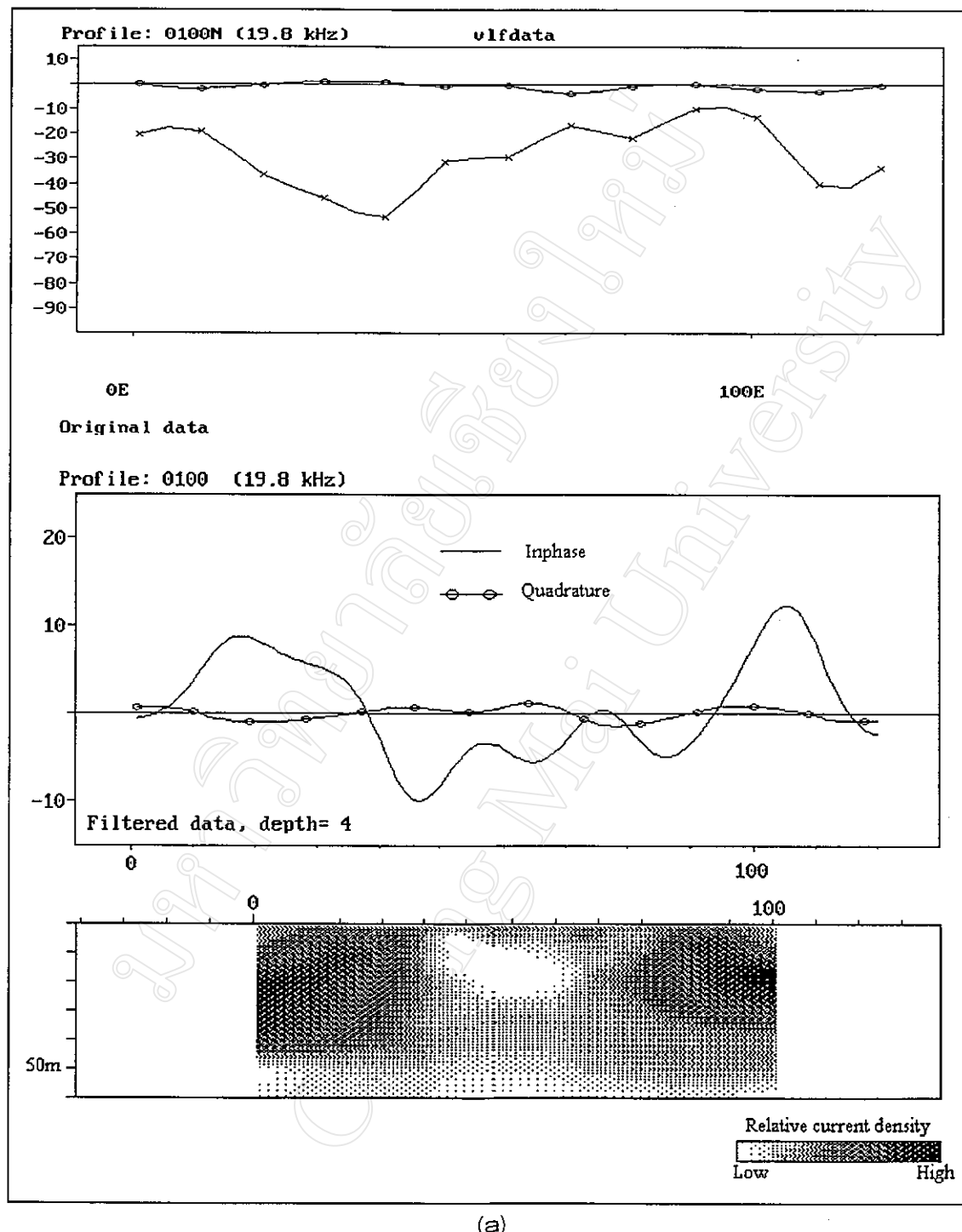


Figure 4.12 VLF original data plot, filtered plot and relative current density pseudosection of (a) profile 100, (b) profile 600, (c) profile 700, (d) profile 800, and (e) profile 900.

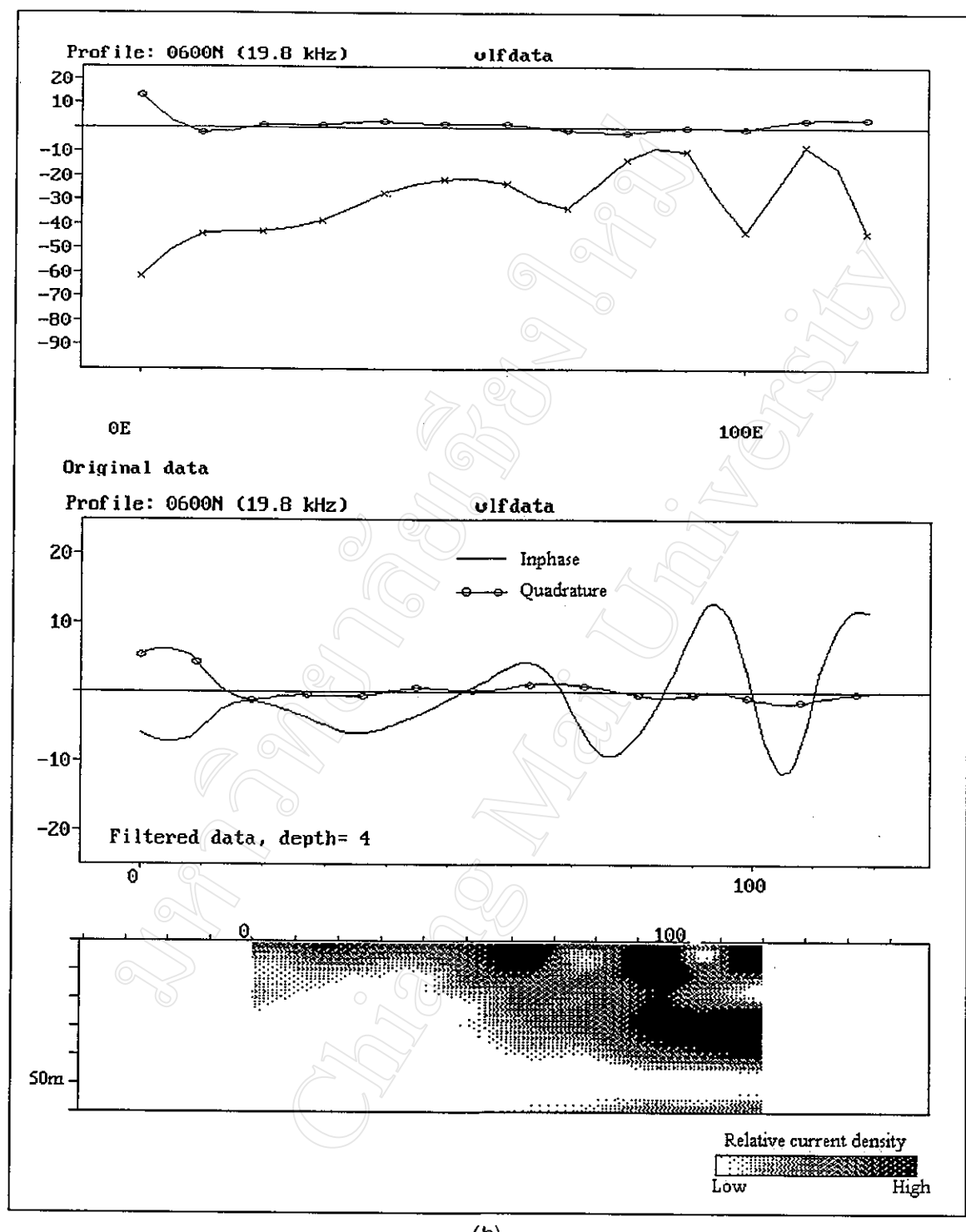


Figure 4.12 (continued).

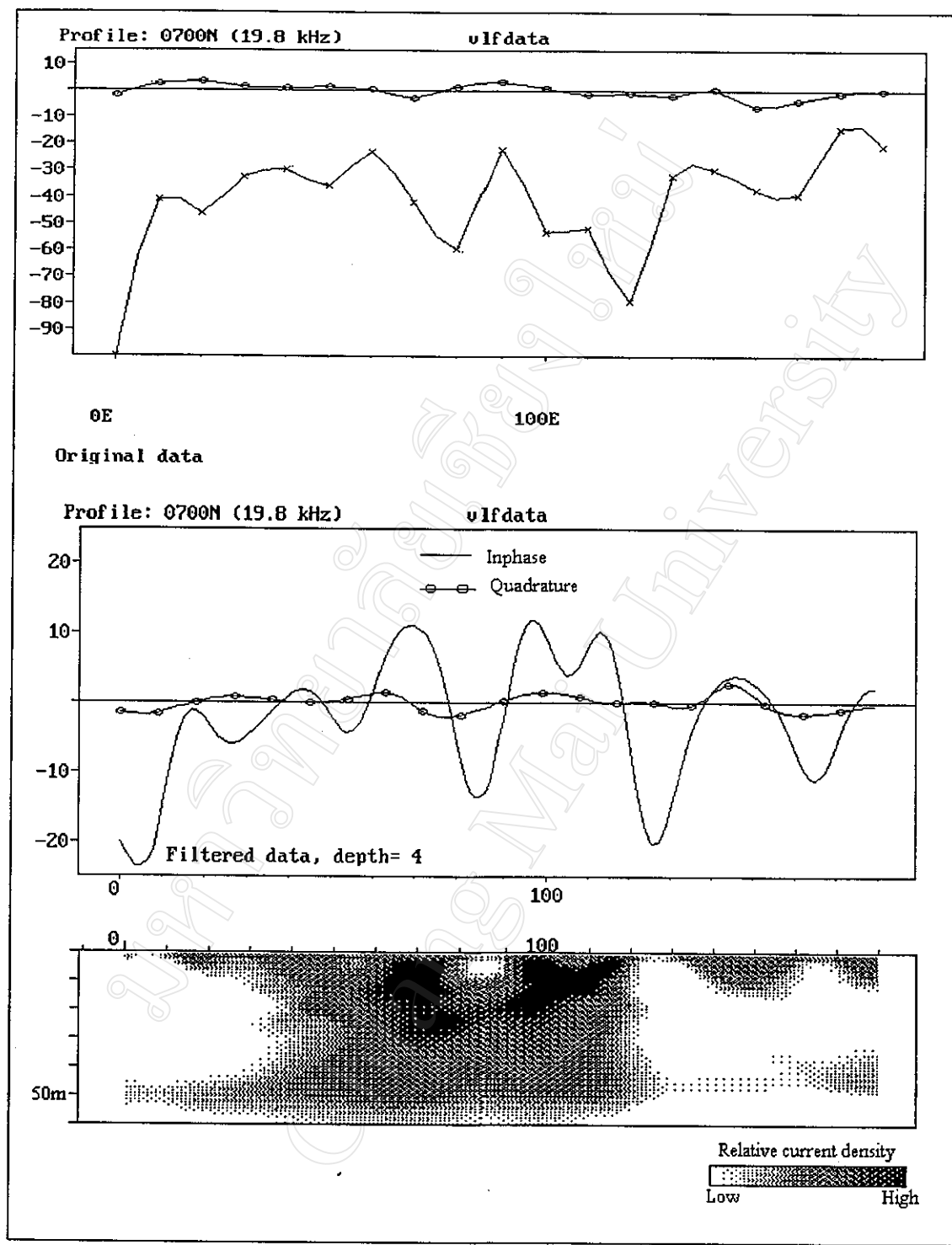


Figure 4.12 (continued).

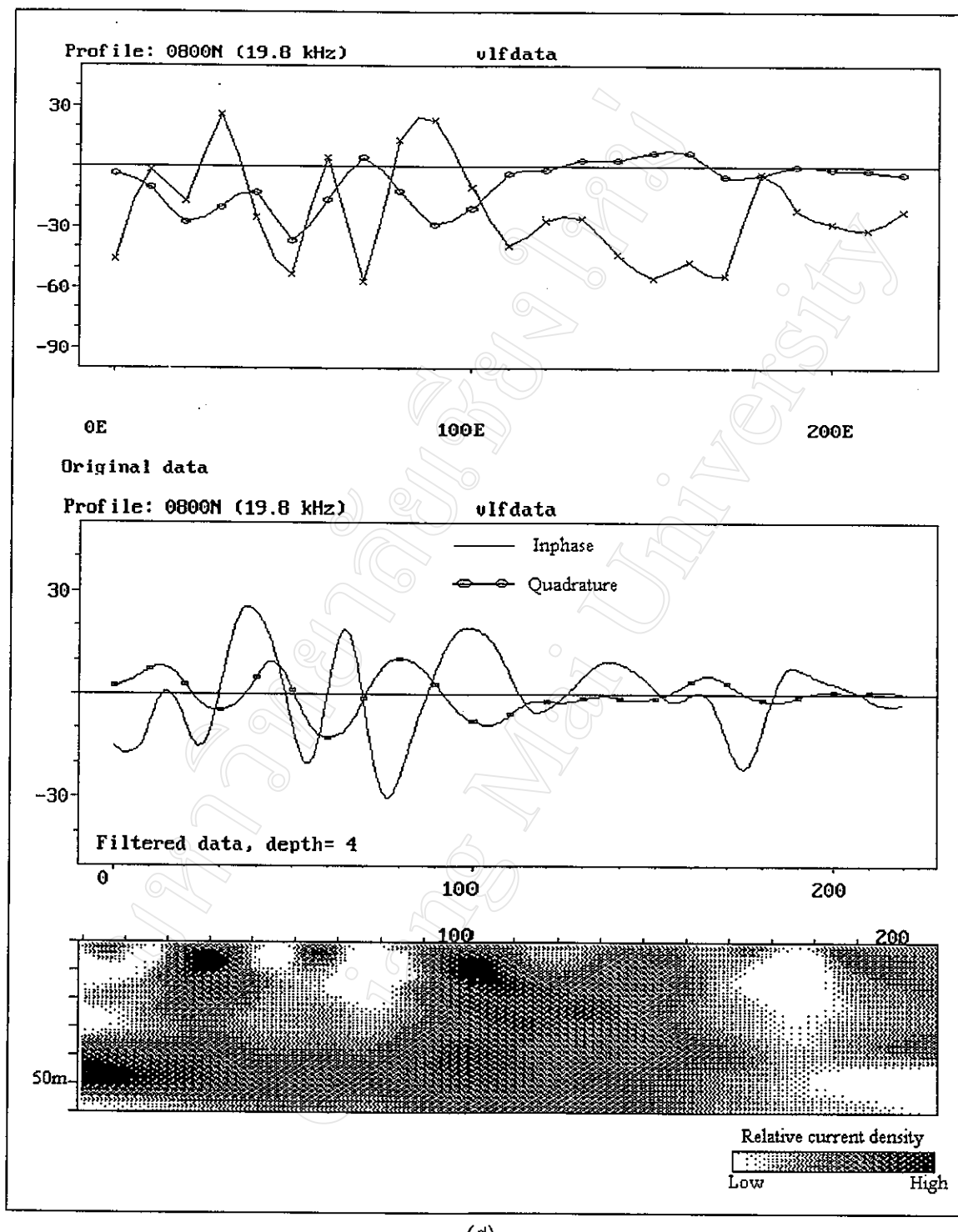


Figure 4.12 (continued).

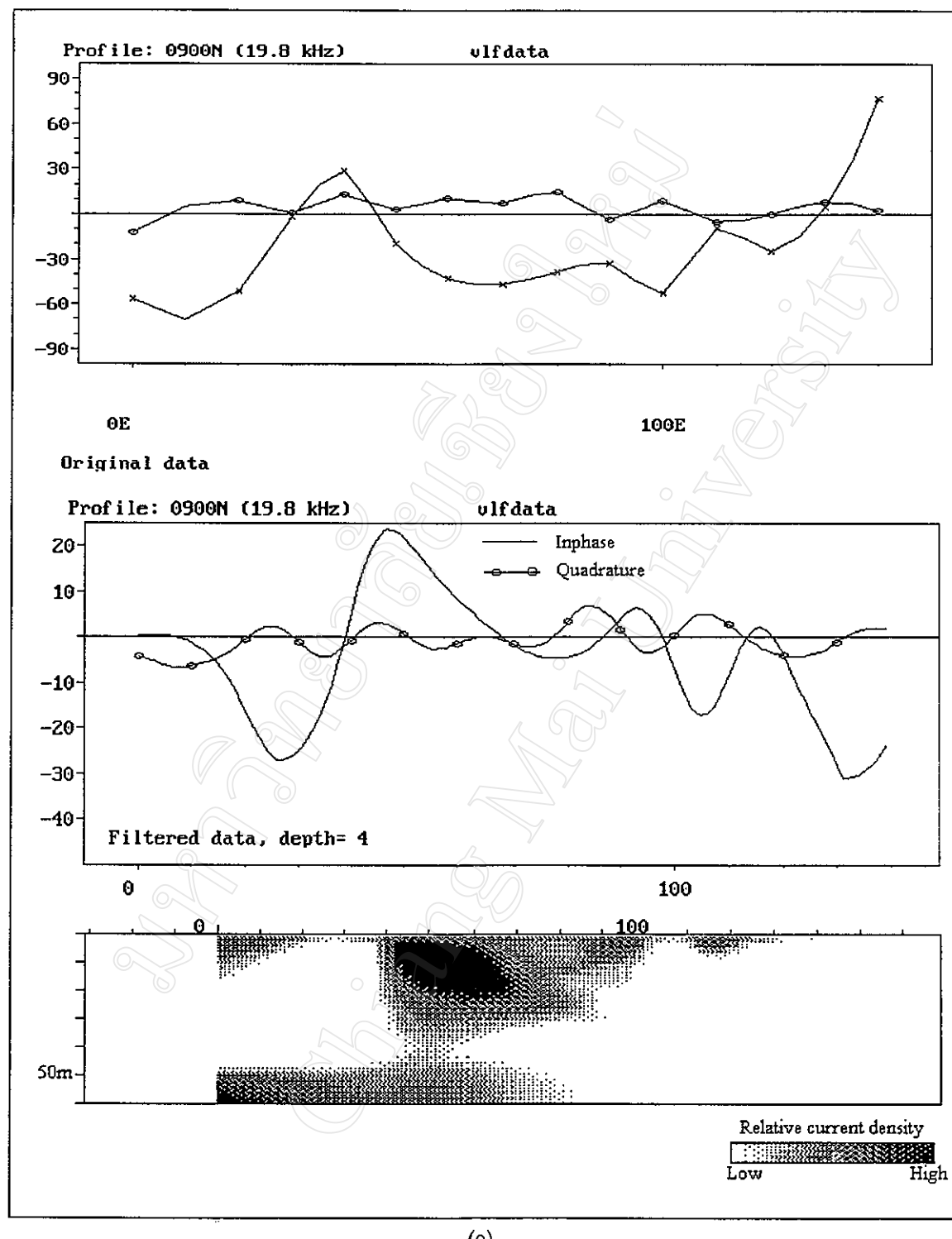


Figure 4.12 (continued).

DD' and current density pseudosection of profile 500, respectively. They are not clearly to interpret.

The combination of resistivity and very low frequency electromagnetic surveys provide indications of the contaminant plume as having low resistivity values. However, this low resistivity zone can not be confirmed as zone of groundwater contamination. For this reason, available hydrochemical data were used to verify the geophysical interpretation. Concentration maps of chloride and total dissolved solids were constructed using data from CMU-JICA (1992), Wisuthitarawong and Prawittarawong (1996) and Karnchanawong *et al.* (1997) to evaluate the groundwater quality.

Figure 4.16 shows the chloride concentration maps in 1989, 1995, and 1997, respectively. The number of data in 1995 and 1997 are less than that of 1989. However, it is obvious that chloride concentration in the eastern part of landfill site 1 increase with time. The total dissolved solids concentration maps show similar results for chloride (Figure 4.17).

Figure 4.18 shows the calculated resistivity maps of shallow well water in 1989, 1995 and 1997, respectively. These calculated resistivity maps agree well with the resistivity maps of geophysical surveys. The chloride and total dissolved solids concentration maps and calculated resistivity maps can indicate that the low values of water resistivity are influenced by high chloride and total dissolved solids concentrations. When compared with resistivity map that obtained from geophysical surveys, the low resistivity zones occur in similar area. However, these calculated resistivity values and the resistivity values derived from geophysical surveys are not similarly because the latter is the resistivity of aquifer materials and groundwater rather than groundwater only. Moreover, the latest hydrochemical data obtained from water samples collected in 1977, while this study obtained from geophysical survey in 2000.

The contaminated area as interpreted from geophysical surveys is shown in Figure 4.19. The contaminant plume underlies the landfill. It is about 200 to 400 meters wide, and may migrate eastward and northeastward. There is a trend of narrower contaminant plume migrates southeastward along with small stream. Many intermediate and high resistivity values in the middle and southern parts of the site may indicate that there is no significant contamination of groundwater in these areas.

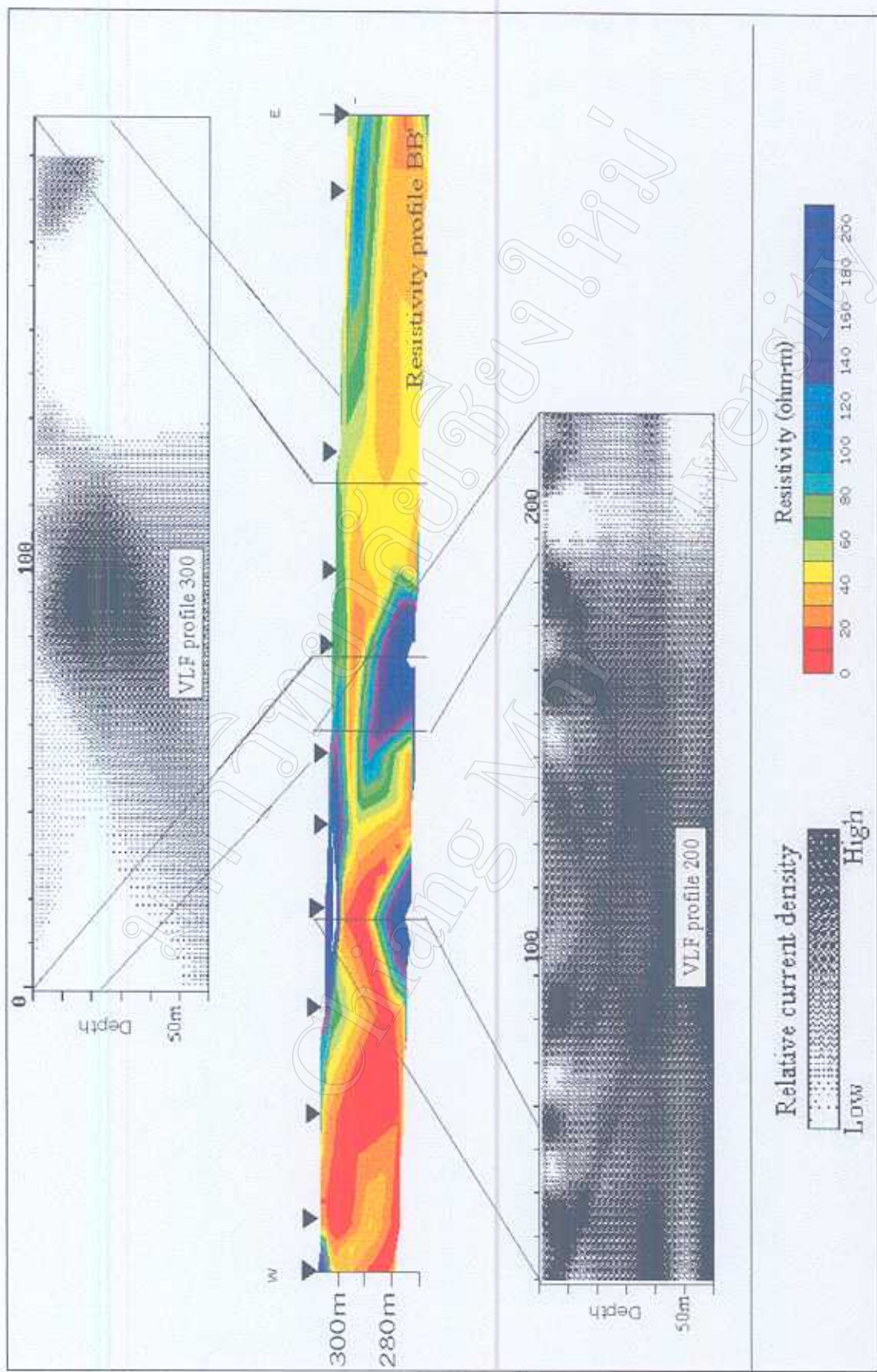


Figure 4.13 Comparison of resistivity profile BB' and current density pseudosections of profile 200 and 300.

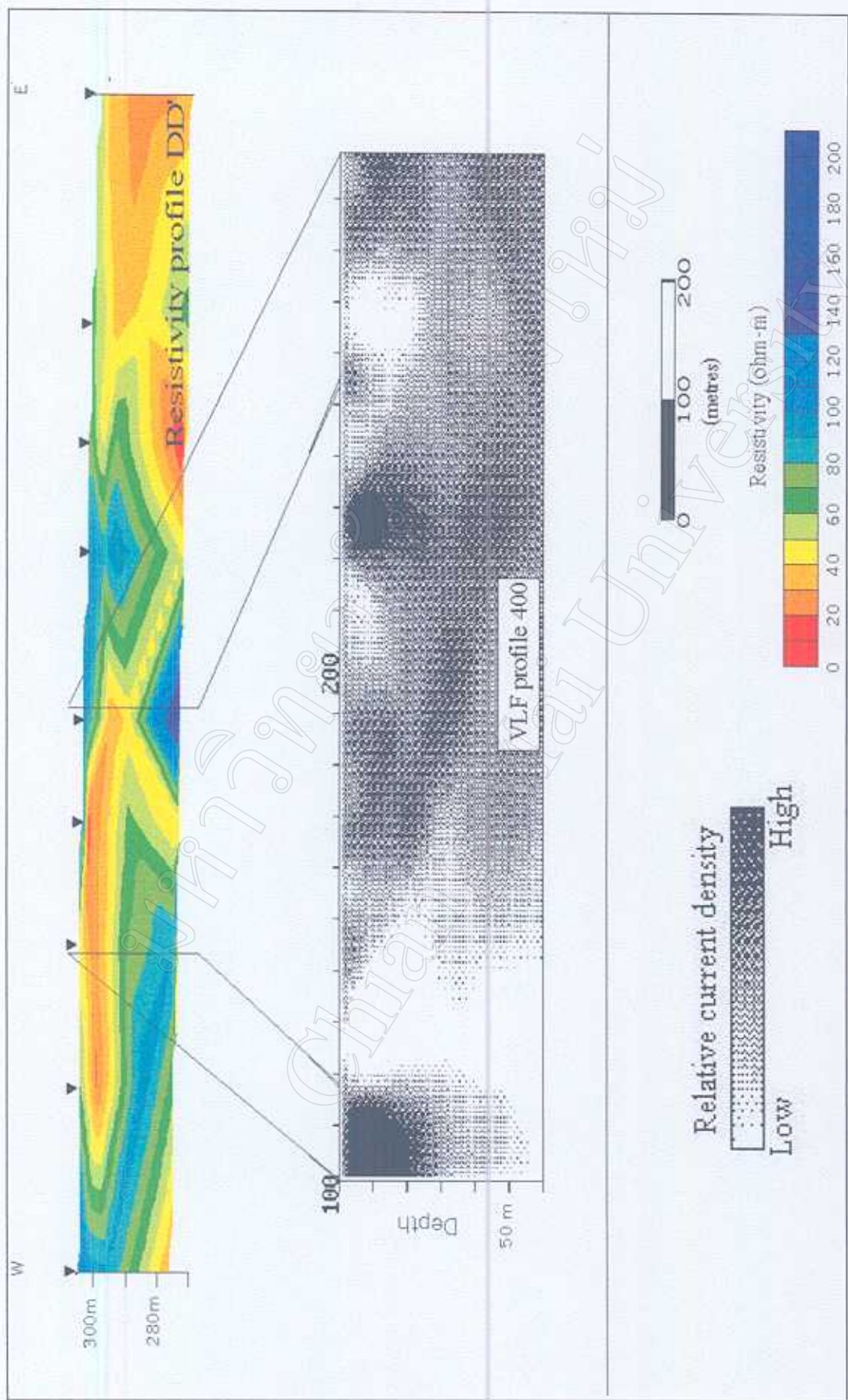


Figure 4.14 Comparison of resistivity profile CC' and current density pseudosection of profile 400.

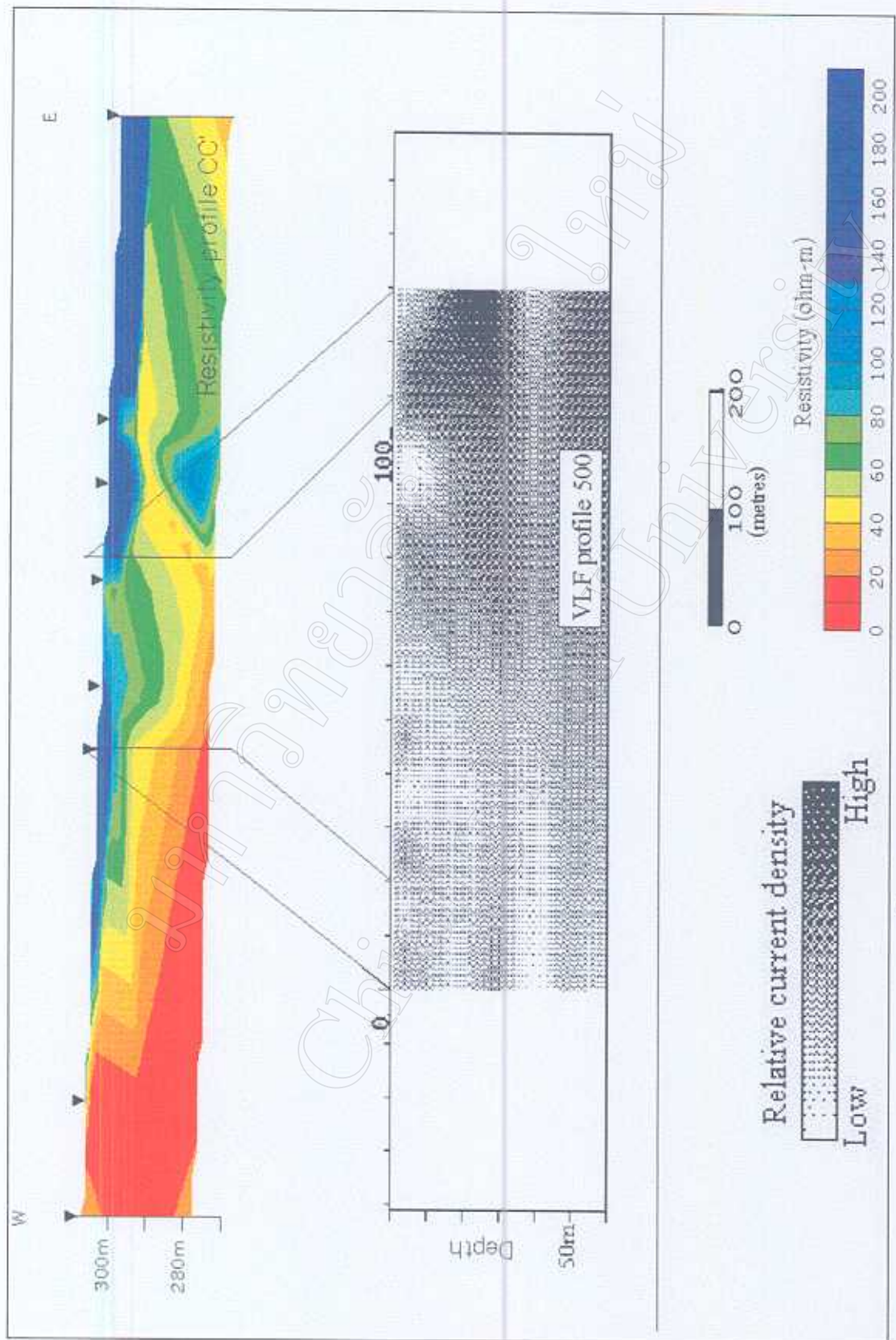


Figure 4.15 Comparison of resistivity profile  $DD'$  and current density pseudosection of profile 500.

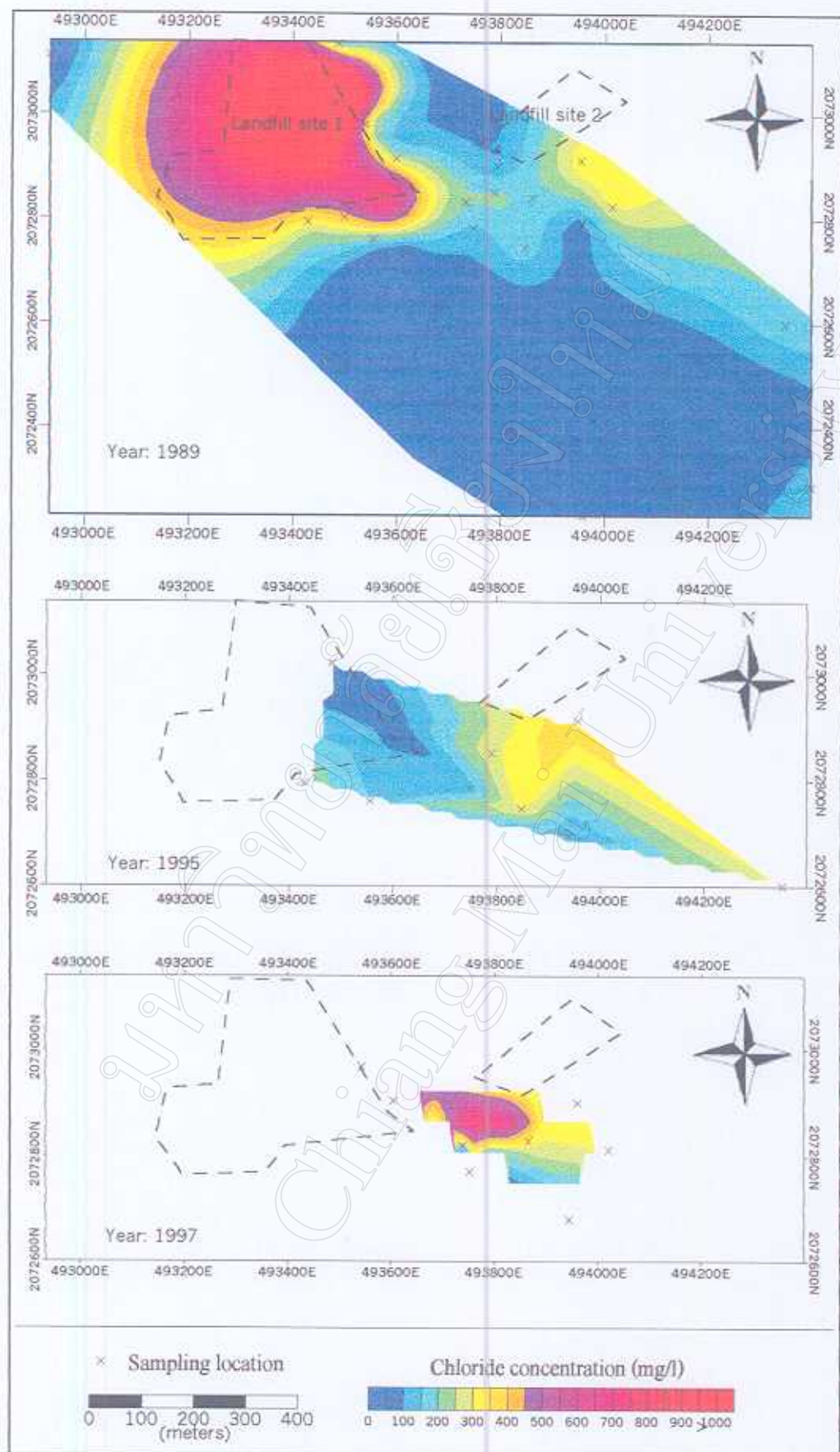


Figure 4.16 Chloride concentration maps of shallow well water (data from CMU-JICA, 1992, Wisuthitarawong and Prawittarawong, 1996, and Karnchanawong *et al.*, 1997).

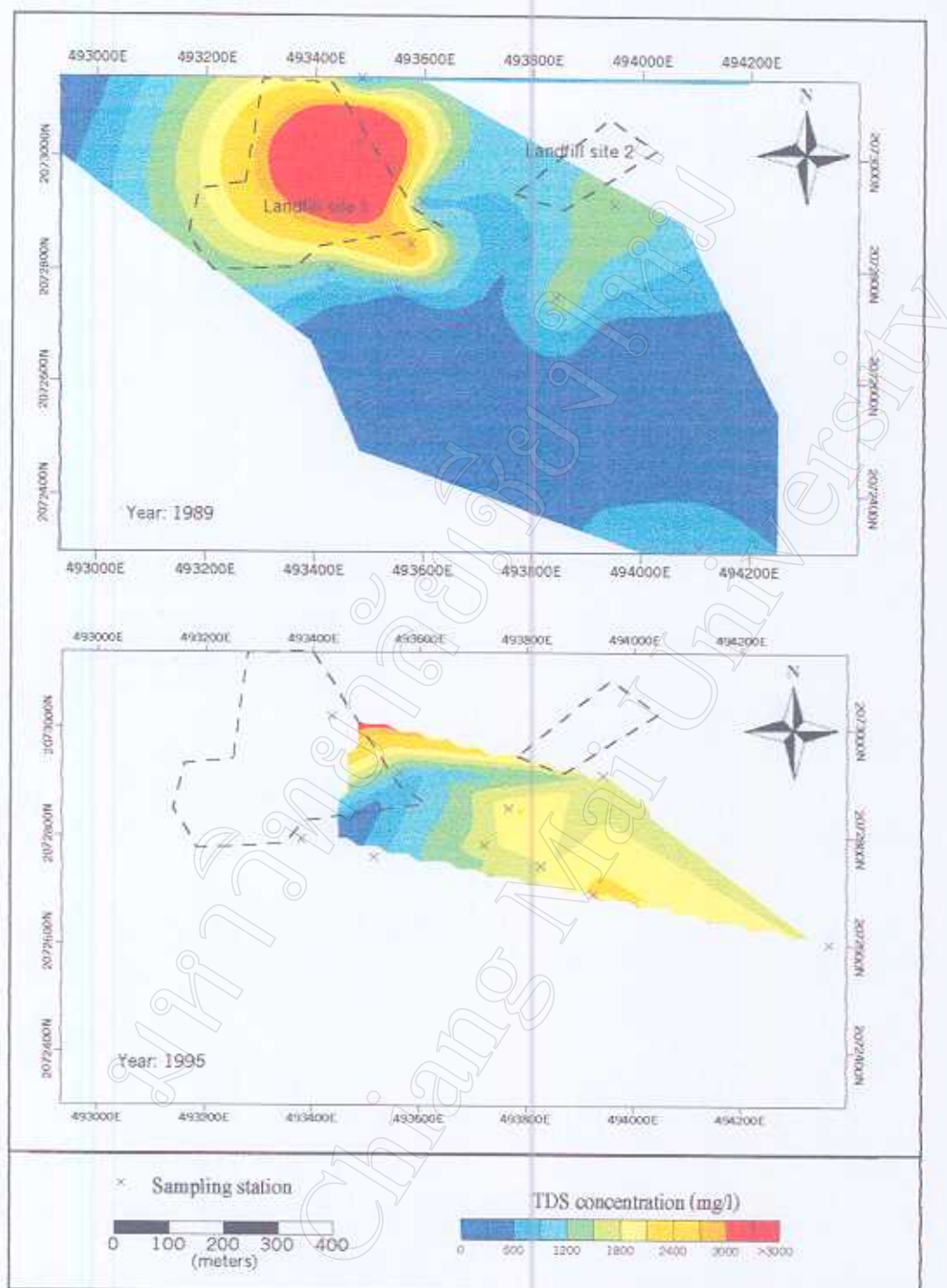


Figure 4.17 Total dissolved solids concentration maps of shallow well water

(data from CMU-JICA, 1992, Wisutitarawong and Prawittarawong, 1996, and Karnchanawong *et al.*, 1997).

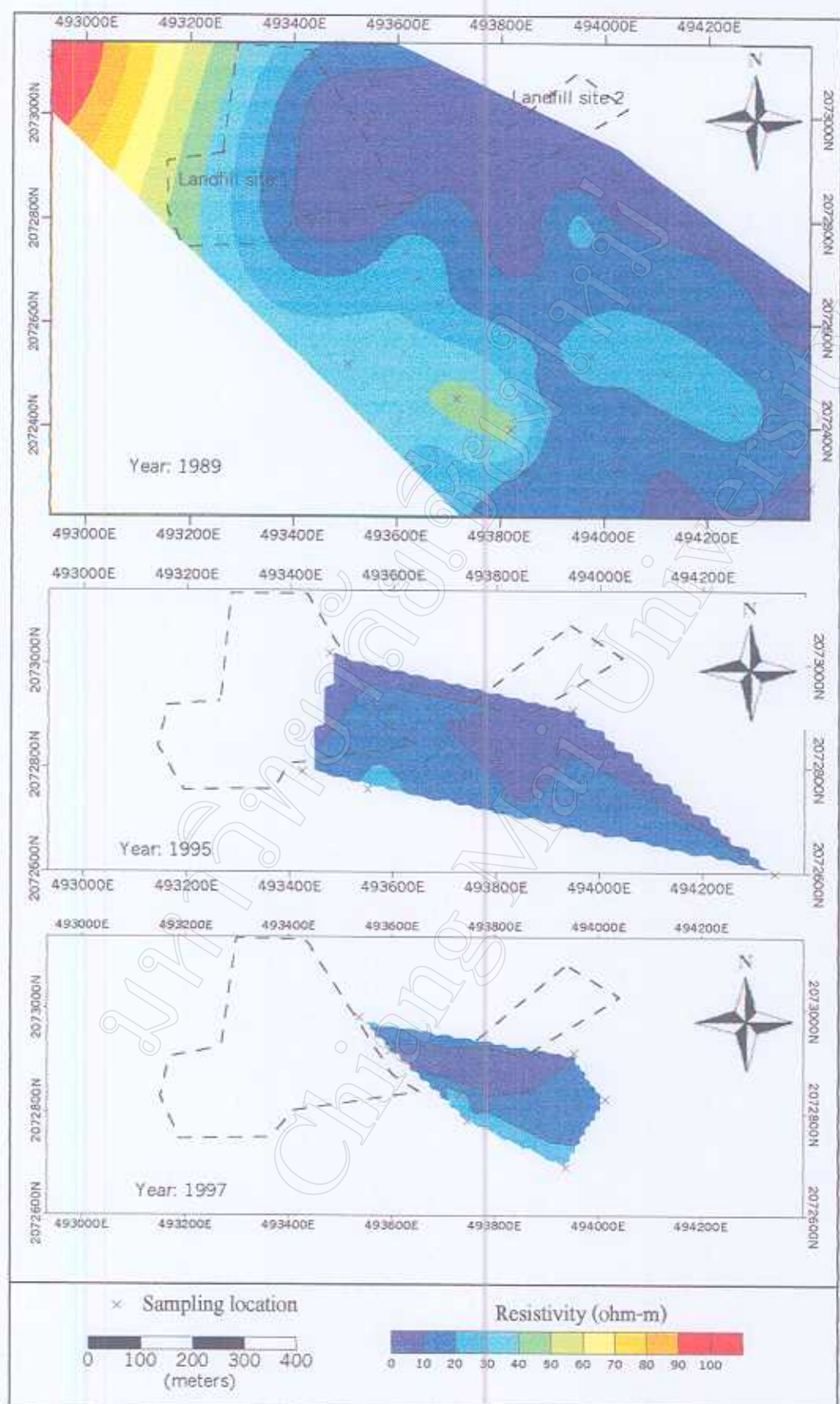


Figure 4.18 Resistivity maps of shallow well water (data from CMU-JICA, 1992, Wisuthitarawong and Prawittarawong, 1996, and Karnchanawong *et al.*, 1997).

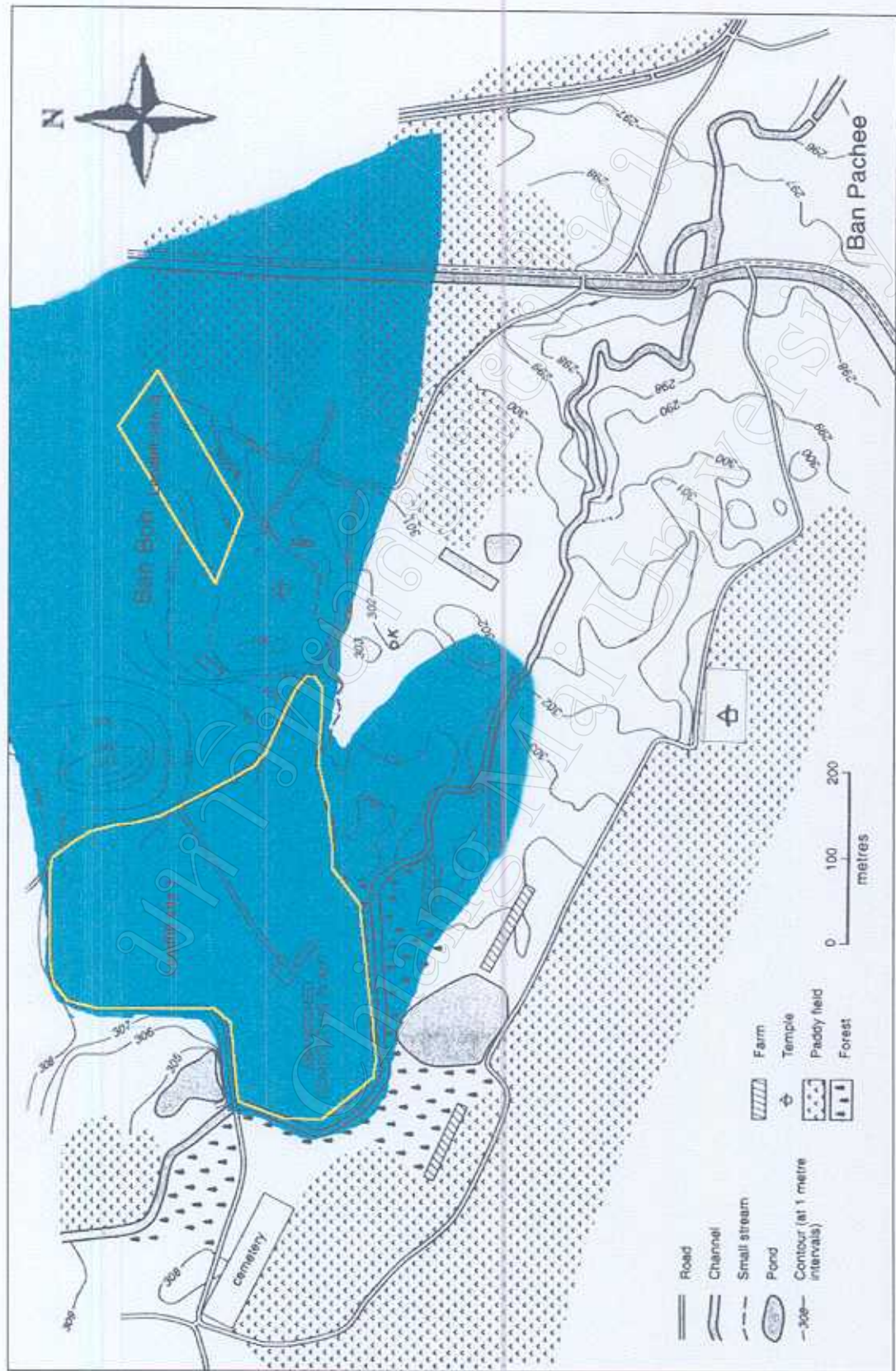


Figure 4.19 Map showing area of groundwater contamination (blue color represent contaminated area).